Journal of Foraminiferal Research, v. 34, no. 1, p. 49–73, January 2004

LOW-DIVERSITY, LATE MAASTRICHTIAN AND EARLY DANIAN PLANKTIC FORAMINIFERAL ASSEMBLAGES OF THE EASTERN TETHYS

GERTA KELLER

Department of Geosciences, Princeton University, Princeton NJ 08544, USA
Email: gkeller@princeton.edu

ABSTRACT

The eastern Tethys, from Israel to Egypt, experienced unusually adverse environmental conditions for planktic foraminifera during the last two million years of the Maastrichtian, as evident by very low species richness, blooms of opportunistic *Guembelitria* species in surface waters, dominance of low-oxygen-tolerant heterohelicids in subsurface waters, and near absence of deeper dwelling globotruncanids. Comparison of southern Israel (Mishor Rotem section) with central Egypt (Gebel Qreiya section) reveals that adverse conditions intensified towards the south with foraminiferal assemblages mimicking stress conditions of the early Danian, dominated (75–90%) by *Guembelitria* blooms. Faunal assemblages indicate an expanded oxygen minimum and dysoxic zone throughout the region, though at the greater depths represented by localities of southern Israel, bottom waters remained aerobic. Primary productivity was extremely low, as indicated by stable isotopes and low total organic content in sediments. These adverse environmental conditions are likely related to the regional paleobathymetry of the tectonically active Syrian Arc that spans Syria to Egypt. The paleorelief of intra-shelf and intra-slope basins of the Syrian Arc, with their differential rates of subsidence and sedimentation, active folding and faulting, likely controlled the intensity of circulation, upwelling, watermass stratification and the extent of the oxygen minimum zone. The late Maastrichtian rapid climate and sea level changes exacerbated these conditions.

INTRODUCTION

The recognition of major paleoclimatic and paleoceanographic changes during the late Maastrichtian has focused new attention on global climate changes and their effect on marine organisms. In particular, the last half million years of the Maastrichtian is increasingly recognized as a time of rapid and extreme climate changes characterized by maximum cooling at about 65.5 Ma, followed by 3–4° C greenhouse warming and major Deccan volcanic activity between 65.4 and 65.2 Ma (Barrera, 1994; Courtillot and others, 1996; Li and Keller, 1998a; Hoffmann and others, 2000; Keller, 2001). The effects of the resultant long-term environmental instability have now been recognized by many planktic foraminiferal workers (Abramovich and others, 1998; Kucera and Malmgren, 1998; Li and Keller, 1998b, c; Olsson and others, 2001; MacLeod and others, 2001; Keller, 2001; Abramovich and Keller, 2002). The biotic effects range from diversity and species abundance changes to local disappearances, and in the most extreme case, mimic early Danian *Guembelitria*-dominated assemblages, as recently observed in late Maastrichtian sediments of central Egypt (Keller, 2002), Bulgaria (Adatte and others, 2002a) and Madagascar (Abramovich and others, 2002).

Until recently, a major pulse in Deccan volcanism and CO_2 release between 65.4–65.2 Ma (Courtillot and others, 1996; Hoffmann and others, 2000) seemed the most likely cause for the greenhouse warming (Kucera and Malmgren, 1998; Li and Keller, 1998a) and associated biotic effects. But the recent discovery of glass spherule layers in upper Maastrichtian marls of northeastern Mexico suggests that a late Maastrichtian impact (or comet shower) may also have played a critical role in destabilizing the environment (Keller, 2001; Keller and others, 2002a, 2003). Three to four glass spherule layers have been reported interbedded with up to 10 m of upper Maastrichtian marl of the Mendez Formation in many localities in northeastern Mexico, with the stratigraphically oldest spherule layer predating the K/T boundary by about 270–300 thousand years, suggesting a pre-K/T impact event followed by reworking of spherules, or a comet shower (Keller and others 2002a, 2003). Recently, Ellwood and others (2003) reported an Ir anomaly also from the uppermost Maastrichtian 1.3m below the K/T boundary and suggested a pre-K/T impact.

Three late Maastrichtian layers of "microspherules of different colors and chemical compositions" of possible impact origin were also reported from the Mishor Rotem section at Makhtesh Gadol in the Negev of Israel by Rosenfeld and others (1989, p. 474). This report led us to examine this section in an effort to determine the age and geochemical similarity of these spherule deposits, compare them with those in Mexico, and evaluate the associated biotic effects. The presence of impact spherules could not be confirmed (Adatte et al., written communication, 2002), though planktic foraminiferal assemblages reveal adverse paleoenvironmental conditions akin to those observed in central Egypt (Keller, 2002). This study documents the biostratigraphy and faunal turnover of the Mishor Rotem section, correlates and compares this section with the Qreiya section of central Egypt, and suggests a model for the observed high-stress assemblages of the region.

LOCATION AND PALEOGEOGRAPHIC SETTING

The Mishor Rotem section is located approximately 10 km north of the Oron phosphate mine on the road towards Dimona (Israel coordinates 1548/0416). The outcrop is on the Rotem syncline east of the Hatira anticline (Figs. 1a,b). This syncline is part of the Syrian Arc structural province of northeast trending gentle folds, which began in the Santonian and continued into the Tertiary (Bosworth and others, 1999; Rosenthal and others, 2000). During the late Maastrichtian, the anticlines and synclines were completely submerged in outer neritic to upper bathyal depths (300–500 m), as indicated by diverse benthic foraminiferal assem-

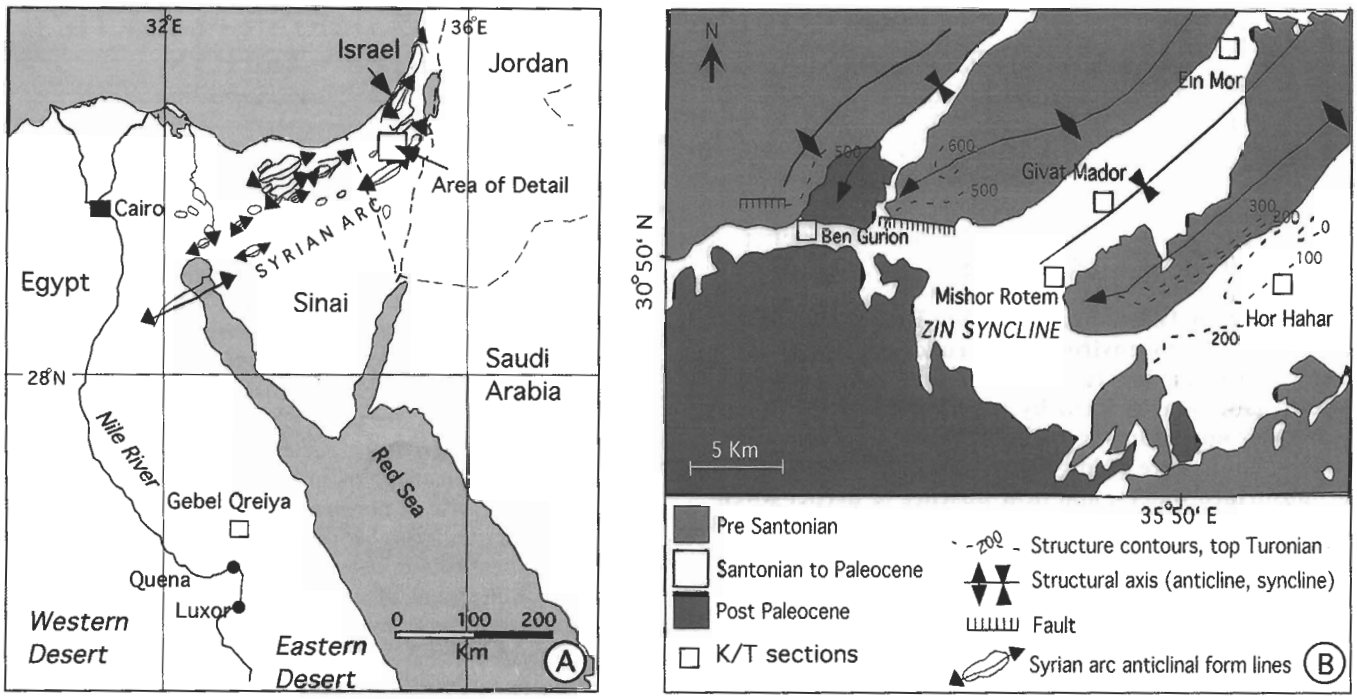

FIGURE 1. A. Location map and tectonic setting of the eastern Tethys showing geography of the Syrian arc and the locations of Mishor Rotem in southern Israel and Qreiya in central Egypt (modified after Bosworth and others, 1999). 1B. Detail of area in the Negev showing structural trend of anticlines and synclines (modified after Magaritz and others, 1985), and localities of upper Maastrichtian to lower Danian sections.

blages (e.g., *Cibicidoides succeedens, C. pseudoacutus, C. hyphalus, Alabamina midwayensis, Angulogavelinella avnimelechi;* see also Speijer, 1994). The section is characterized by three distinct red layers that are interbedded in upper Maastrichtian chalk and marl (Fig. 2). Additional outcrops containing these red layers can be traced laterally along the hillside, as well as to the south in the areas of Givat Mador, Hor Hahar and Ein Mor (Fig. 1b). Sediments are rich in planktic and benthic foraminifera, ostracods, fish debris and occasional brachiopods. In the region of the Rotem syncline (Makhtesh Gadol) the Maastrichtian Ghareb Formation reaches a thickness of 60–80 m and consists of chalk, marly limestone and marl.

The Qreiya section is located in the Asyut Basin of central Egypt and near the southern end of the Syrian arc structural province (Fig. 1a). During the late Maastrichtian to early Paleocene, the section was submerged at middle to outer neritic depths and was subject to sea level fluctuations (Hendriks and others, 1987; Luger and Gröschke, 1989; Speijer, 1994). Paleoenvironmental analyses of this section based on mineralogic, stable isotopic and foraminiferal analyses are published in Keller and others (2002c) and Keller (2002). In this study the planktic foraminiferal assemblages of the Qreiya section are compared with those of the Mishor Rotem section.

METHODS

In the field, the section was trenched to obtain fresh, unweathered sediment samples, which were collected at 10-cm intervals and at closer sample intervals across the red layers and K/T boundary. The section was measured and examined with respect to lithologic changes, bioturbation, macrofossils, sedimentary structures, erosion surfaces and undulating contacts. Samples were processed for foraminiferal analysis following the standard method of Keller and others (1995). Age and biostratigraphic control are based on quantitative planktic foraminiferal analysis of sample splits of about 300 specimens of the >63 μm and >150 μm size fractions. This allows evaluation of both small and large species populations. Species richness evaluation is based on the presence of the total number of species in each sample from both size fractions, as well as rare species (labeled "x" in Tables 1–3) detected in a search of the uncounted residue of each sample. Dominant species are illustrated in Plates 1–2. Foraminifers are relatively well preserved morphologically, but test shells are recrystallized and commonly infilled with blocky calcite or silica. The section is thus not suitable for stable isotope analyses. Planktic foraminiferal microslides are deposited in the Geosciences Micropaleontology Repository of Princeton University.

LITHOLOGY

In the region of Makhtesh Gadol, the Maastrichtian Ghareb Formation reaches a thickness of 60–80 m and consists of white-tan to yellow chalk and marly limestone that form resistant beds, separated by thin layers of laminated red marl stained by iron oxides. Sediments are rich in planktic and benthic foraminifera, ostracods, fish debris and occasional brachiopods. At the Mishor Rotem section, the upper Maastrichtian exposure of the Ghareb Formation consists of about 9 m of horizontally stratified white, tan or yellow bioturbated chalk and marly limestone that form resistant beds, separated by three prominent thin layers of laminated red marls stained by iron oxides (Fig. 2). The overlying Taqiye

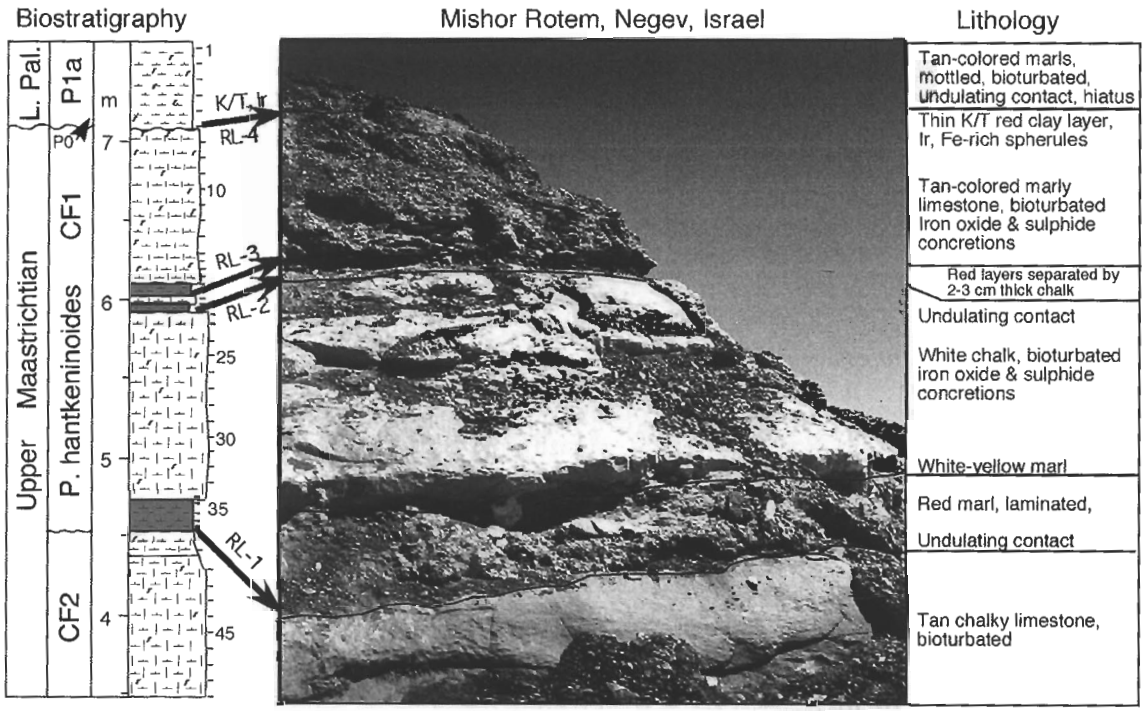

FIGURE 2. Photo of the Mishor Rotem outcrop showing the three red marl layers interbedded with chalk and limestone beds, along with the lithologic column and sediment description. Note that the Ir anomaly of 0.65 ng/g (Rosenfeld and others, 1989; Adatte and others, in press) at the K/T boundary is associated with a red clay layer (RL-4) infilling depressions of an undulating erosion surface. Three red marl layers and the K/T boundary red layer are marked red layers 1–4 (RL-1 to RL-4).

Formation is of Paleocene age and consists predominantly of marls that reach a thickness of about 40–50 m. For this study, the topmost 7 m of the Ghareb Formation and basal 50 cm of the Taqiye Formation were sampled.

The lower 3.5 m of the section consist of bioturbated yellow marl, followed by a 1-m-thick, resistant, bioturbated, tan-colored, chalky limestone. An undulating surface marks the contact between the chalky limestone and overlying 10-cm-thick laminated red marl (labeled RL-1) that is enriched in Pd and Ir (Fig. 2, Adatte and others, written commun., 2002). The red layer grades into bioturbated, white-yellow marl with flaser-bedding and is followed by a 1.2-m-thick, resistant, white, bioturbated chalk rich in iron oxide and sulphide concretions. Two thin (5 cm) red layers (RL-2 and RL-3) separated by a 2–3-cm-thick chalk are between the white chalk and overlying 2-m-thick, tan, marly limestone. The lower red layer (RL-2) is also enriched in Pd and minor Ir, similar to RL-1. A 2-m-thick, tan, marly, bioturbated limestone with iron oxide and sulphide concretions and bounded by erosional surfaces, separates the third red layer (RL-3) from the K/T boundary (RL-4, Fig. 2).

The upper surface of this unit marks the K/T boundary and top of the Ghareb Formation. The dark clay that characterizes the K/T boundary in most complete sections is not present at Mishor Rotem, nor has it been reported from other sections in Israel due to a K/T unconformity (Rosenfeld and others, 1989; Keller and Benjamini, 1991; Abramovich and others, 1998; Speijer, 1994). A hiatus is also present at Mishor Rotem, as observed by the undulating erosional contact at the top of the Maastrichtian tan limestone. However, the characteristic thin K/T red layer (2–4 mm thick, labeled RL-4) is present, though discontinuous, in depressions of the undulating erosional surface of the underlying limestone and contains a small Ir anomaly of 0.6 ng/g (Fig. 2) that was reported by Rosenfeld and others (1989) and Adatte and others (in press). This red layer also contains Fe-rich spherules (Fig. 3) that are commonly found at this boundary in Tunisia, Spain and elsewhere (Smit, 1999). Mottled and bioturbated, tan marl of the Taqiye Formation marks the overlying lower Paleocene.

Spherules in Red Layers

Rosenfeld and others (1989) reported abundant silica-rich microspherules (100–150 μm in diameter) of possible impact origin in the three late Maastrichtian-age red layers. They described the spherules as translucent yellow with K-Al-feldspar compositions, dull brown and green parts composed of Mg-Fe-Al silicates with high FeO concentrations (17–20%), and black parts with >50% Fe_2O_3, 29% SiO_2 and 12% NiO. Although abundant spherules were also recovered from the red layers in this study, no spherules of impact origin could be confirmed (see also Adatte and others, in press). The translucent yellow spherules observed in this study represent largely the silica infilling of foraminiferal chambers, followed by dissolution of the shell carbonate and break-off of individual chambers. Small areas of chamber attachments can be recognized on many spherules. Similarly, many green spherules represent glauconite chamber infillings or glauconite grains, which are common throughout the section. There are also dull brown Fe-rich spherules, which are probably associated with the iron concretions found throughout the upper part of the section. However, similar Fe-rich spherules and an Ir anomaly of 1

TABLE 1A. Mishor Rotem, Negev, Israel. Relative percent abundance of planktic foraminifera in the lower Danian and upper Maastrichtian (>63μ). x = rare.

Biozone	P1a(2)						Plummerita hantkeninoides CF1				
Sample number	1	2	3	4	5	6	7	8	9	10	11
Sample depth (m)	7.60	7.50	7.40	7.30	7.20	7.10	7.00	6.90	6.80	6.70	6.60
Parvularugoglobigerina alabame	2	2	x	x	x	4					
P. extensa	9	27	28	12	3	3					
P. eugubina		x	x	3	4	2					
P. longiapertura		x	3	12	34	22					
Eoglobigerina eobulloides	2	2	1	2	2	5					
E. edita	5	9	5	2	x	x					
Subbotina triloculinoises	10	26	15	6	1	2					
S. trivialis	1		x		x						
Parasubbotina pseudobulloides	3	8	18	9	x	3					
P. varianta	2										
Woodringina claytonensis	6	x	1	6	1	2					
W. hornerstownensis	9	2	7	1	3	1					
Chiloguembelina midwayensis	1	x	3	18	2	x					
Globanomalina compressa	1	x	1	11	2	x					
G. pentagona	7	6	8	4	x	1					
G. taurica	2		1	1							
Globocunusa daubjergensis	16	4	3	5	3	10					
Guembelitria cretacea	13	3	2	6	5	37	6	12	5	x	1
G. danica	x	x	x	2	x	5					
G. irregularis	2	x	x	1	x	x					
G. trifolia						7	2				
Globigerinelloides aspera	1	x	x	x	x	7	20	21	19	14	16
G. yaucoensis	x	x									
G. rosebudensis					x	2	x	1	x		x
Globotruncanella minuta										1	
G. petalloidea						2	1	3	2	1	2
G. subcarinatus	x			x	x	3	2	2	3	1	
Abathomphalus mayaroensis											
Globotruncana aegyptiaca											
G. arca						x					
G. esnehensis											
Hedbergella holmdelensis				x		x	1	1			2
H. monmouthensis	x				x	x	1	1	1	1	
Plummerita hantkeninoides						x		1	1	x	
Rugoglobigerina hexacamerata									1		
R. macrocephala		x			2	1	1	1	3	2	5
R. pennyi										x	
R. reicheli					x	2	1	1	1	x	
R. rugosa		x	x	x	2	2	2	x	2	1	5
R. scotti						1				x	x
Heterohelix globulosa	x	x	1	x	8	16	10	18	13	19	14
H. globulosa B							4		3	3	2
H. dentata	x	x	1	x	2	3	5	6	10	5	2
H. glabrans					x		5		2	4	
H. labellosa				x	2	3				x	2
H. navarroensis	1		1	x	3	22	11	13	18	20	25
H. planata			x		1	4	6	2			1
H. pulchra									x	2	x
H. punctulata			x		2	x	2	x	1	x	2
Pseudoguembelina hariaensis						x	x				
P. costulata			x	x	2	5	6	7	6	5	5
P. costellifera						3	8	3	7	11	2
P. kempensis						2				x	x
P. palpebra						x	1	x		1	5
Pseudotextularia elegans					2	1	2		2	x	1
P. nuttalli									x		
Planoglobulina carseyae					2	3	2	5	1	3	2
P. brazoensis						x					
Juveniles no ID	2	3	x	x	3	2	x	x	x	2	3
Total counted	401	307	423	409	323	292	408	282	349	374	267

ppb have also been reported from the uppermost Maastrichtian in Oman by Ellwood and others (2003). These authors suggested a pre-K/T impact event, similar to northeastern Mexico (Keller and others, 2002a, 2003).

In addition, we found one type of yellow translucent spherule in the 200–400 μm size range that is present in the basal 0.5 cm of red layers RL-1 to RL-3, but also in the marl interval of sample 58 (Fig. 2). These spherules are

TABLE 1A. Extended.

Plummerita hantkeninoides CF1																				
12 6.50	13 6.40	14 6.30	16 6.20	18 6.10	19 6.05	20 6.00	21 5.98	21a 5.97	21c 5.95	22 5.91	23 5.85	24 5.75	25 5.65	26 5.55	27 5.45	28 5.35	29 5.25	30 5.15	31 5.05	32 4.95
x	5	3	2	3	21	19	21	49	48	14	42	46	33	34	23	30	30	17	20	18
17	19	16	23	5	18	9	8	4	1	x	3	1	3	3	3	7	3	6	8	6
	x																1			
		2	2			x													x	
	x																			
2	x	1	1	x	x	2	1			2		x	x	x	x	x			2	x
x			2	2		2	x			2	x	1	x	x	x			x		
x																				
						x		x												
								x	x									x		
	x	x	x																	
x	x	x		2	2	2	4	x	5	1				1		1	5	2	5	3
1	x			x		2	x	x	x	2	2	1	1	x	2	1		2	x	1
								x												
3	x	1	x	x		1	1	x	2		2	2	1	1	2	1			x	
					x			x			2	x	x		x					
1	1	x	x	2	1	1	x	1	2	x		1	x	1	x	x	x	1		1
1		1					x									x	x	1		
26	17	18	15	21	15	16	12	13	17	29	13	14	20	19	20	17	11	22	19	30
3		4		6					x								6	x		
2	5	10	10	2	8	8	3	3	x	5	5	2	4	3	8	4	5	3	6	7
1	2	2	5		x	x	1	1	x		1	x	x	1	1	1	x	1	2	2
1	x		1		x	1	x						1			2	x	1		2
9	23	21	14	27	15	15	16	12	10	15	10	6	15	11	18	15	20	17	15	11
2		x	1	3	3		3	x	1	3	2	4	3	2	x	2				3
	x	x	2	x	1	1	1				1			1	1	x	1		2	1
2	1				1	2	1	x	x	x	3	6	x	2	1	4	2	x		3
	1		1			1	x			2	x				2					
5	5	6	5	11	3	8	10	5	3	7	2	3	3	4	2	7	4	6	4	2
2	x	3	2	2	1	1	1	2	x	1	2	4	4	4	7	1	3	7	x	5
1	x		1	2	x	1	2	1	3		1	2	1	1	x	x		2		
7	1					1	1	x	1	3		x		2	1	1		1	x	1
7	10	5	7	6	3	2	5	3	2	5	5	3	5	5	4	1	3	5	2	1
						x														
4	2	3	3	1	3	1	5	x	3	4	1	1	1	1	2	3	2	2	2	2
2	3	2	x	3	3	2	1	x	x	2	x	x	2	2	x	x	2	3	1	x
344	416	306	388	242	296	286	354	275	231	239	238	243	268	335	246	285	271	252	312	198

glassy in appearance with smooth surfaces, conchoidal fractures, and frequently zoned outer rims (Fig. 3). Some spherules have residual calcite crystals on the outer surface or on broken fragments; others have tiny air bubble inclusions. The chemical composition of some spherules is almost pure carbon (~90–95%), whereas others are high in sulfur. These spherules appear to be amber. Similar spherules have been observed from upper Cretaceous sequences in Jordan, Leb-

TABLE 1B. Mishor Rotem Negev, Israel. Relative percent abundance of planktic foraminifera in the upper Maastrichtian (>63). x = rare.

	CF1						CF3					
Biozone												
Sample number	33	34	35	36	37	39	40	41	42	43	44	45
Sample depth (m)	4.85	4.75	4.71	4.65	4.60	4.50	4.40	4.30	4.20	4.10	4.00	3.90
Guembelitria cretacea	15	10	x	2	1	2	1	1	10	12	12	1
G. danica		x										
G. trifolia												
Globigerinelloides aspera	4	10	2	6	4	7	1	4	9	9	12	5
G. yaucoensis		x			x				2	1	x	
G. rosebudensis	x									x		
Globotruncanella minuta												
G. petalloidea		1				1		1	2		5	2
G. subcarinatus			x	2	1	x	1		2	4	6	2
Abathomphalus mayaroensis												
Globotruncana aegyptiaca				x	x							x
G. arca												
G. esnehensis					x			x				
Globotruncanita conica											x	
G. pettersi				x				x				
G. stuarti												
Hedbergella holmdelensis		x		1					2		x	
H. monmouthensis	1	2		1	x	1		1	1	1	3	
Plummerita hantkeninoides	1		1	1		x						
Rugoglobigerina hexacamerata												
R. macrocephala	1	2	2	3	4	2	2	2	3	2	1	5
R. pennyi												
R. reicheli		1		x		x	2	2	x			
R. rugosa	x	x	x	x	1	x	2	x	x	2		x
R. scotti		x	x	1	2		1	x	x	x	x	x
Heterohelix globulosa	19	18	21	19	11	19	11	16	9	17	7	4
H. globulosa B	5	7	11	9	19	x	12	10	12	9	8	38
H. carinata												
H. dentata	5	6	1	5		6	7	3	4	4	8	4
H. glabrans	2	4		1	3	2	2	1	3	1	3	4
H. labellosa		x		1		x	1	3		1		
H. moremani												
H. navarroensis	15	21	6	11	8	13	3	10	15	10	8	5
H. planata	2	2	7	x	1	2	6	2		2		
H. pulchra	1	2	x	x	2	x					1	x
H. punctulata		2	4	3	6	x	3	1		1	1	2
H. cf. *punctulata*												
Pseudoguembelina hariaensis	3	x	1	2	1	x	2					
P. costulata	6	3	11	5	10	15	10	9	11	5	7	9
P. costellifera	10	4	8	7	11	14	13	16	12	10	10	4
P. kempensis		1	2	1	2	x	1	2		x	x	x
P. palpebra	3	x	2	1	x	1	4	1	1	1	2	1
Pseudotextularia elegans	4	1	11	8	8	6	11	7	x			3
P. nuttalli				4		x	x					
Planoglobulina carseyae	1	1	3	4	3	2	1	4	x	3	1	6
P. brazoensis					x						x	
P. multicamerata				x								
Juveniles no ID	x	x	3	x	x	2	2	x	x	2	1	2
Total counted	215	278	190	252	228	298	148	284	248	222	225	141

anon and Syria, where they were derived from Araucaria forests (Bandel et al., 1997).

BIOSTRATIGRAPHY

The Mishor Rotem section of the Makhtesh Gadol area of the Negev is the first locality in Israel where a thin K/T boundary clay layer with spherules and Ir anomaly has been found (Rosenfeld et al., 1989; Adatte and others, in press). In other published localities throughout southern Israel, the K/T boundary clay and most of the basal Danian is missing due to erosion (Magaritz and others, 1985; Rosenfeld and others, 1989; Keller and Benjamini, 1991). To evaluate the nature and continuity of the sedimentary record, the biostratigraphy is here evaluated based on the early Danian zonal scheme by Keller and others (1995) and the Cretaceous foraminiferal (CF) zonal scheme by Li and Keller (1998a, b) which replaces the *Abathomphalus mayaroensis* zone with four zones for a much improved age control for the late Maastrichtian (Fig. 4). Age estimates for late Maastrichtian biozones are based on foraminiferal datum events of DSDP Site 525 and Agost, Spain, tied to the paleomagnetic stratigraphy of the same sections (Pardo and others, 1996; Li and Keller, 1998a). Ages for these Maastrichtian and Danian datum events and biozones are broadly valid for the eastern Tethys region (Fig. 5).

Zone CF3. The late Maastrichtian Zone CF3 defines the interval from the first appearance of *Pseudoguembelina*

TABLE 1B. Extended.

CF3																				
46 3.80	47 3.70	48 3.60	49 3.50	50 3.40	51 3.30	52 3.20	54 3.00	56 2.80	58 2.60	60 2.40	62 2.20	64 2.00	66 1.80	68 1.60	70 1.40	72 1.20	74 1.00	76 0.80	78 0.40	80 0.20
	3	5	16	22	23	16	36	18	18	7	x	x	22	21	22	4	6	6	7	5
																				x
4	13	1	3	8	9	8	6	10	5	5	6	4	8	7	10	8	5	3	10	5
	2			1												1	1	2	1	x
1	1			x	1		2	2	x	x	1	3	1	1	1			2	x	2
				x									1	2		x	3		2	
2	x	x		1	1	x		x			x	x	2	3	2	2	x	1	2	2
1	5	1	2		5	3	2	5	5	1	5	4	5	2	2	2	4	5	2	2
x																				
x																				
x																				
x	1	1				1						2				x				1
		2	2	3		x	3	1	1	x		1	x	1	2	1	2	4	3	3
5	x	6	3		1	1		2	2	2	2	4	6	1	2	1	2	1	3	1
3	4	1	x	1	1		1	1	x		1	1	x	x			x	x	1	1
2	1	x	x						x		x		x	x				1		
5	11	13	6	7	8	13	9	11	19	14	14	14	7	10	12	18	14	19	15	12
26	20	30	30	7	9	16	5	6	11	12	16	17	8	10	10	9	21	7	15	8
																	x			
1	5	4	x	5	7	8	5	8	5	11	7	10	2	5	7	3	9	7	8	12
3	4	2	x	3	3	3	5	2		2	1	5	1	2	2	3	x	3	3	x
3			x		x	1								x		x				
3	x	1		x		2	2	2	4				5	3		x	4	x	1	1
7	10	15	10	19	22	16	21	22	20	27	24	22	19	25	18	29	19	26	18	30
									2	3	4									
	2	x			x	x		3	1	1	1	1	x	x	1	x	2			
1	x	3	6	2	x	x		1		1	1	x	x			1	1		x	1
x		x				x										x			x	x
5	7	2	14	12	7	8	3	4	5	12	14	8	9	5	5	12	5	6	7	8
4	3	4																		
1		x	1																	
2	2		2		x	x						1	x	1					x	x
5	1	1	x							x	x							x	1	
1	2			x								1			x			1		1
4	x	7	4			1		x	1		1				x	2		1		2
x																				
2	x	x	x	2	x			x	x	2	x	1	1		1	2	1	2	1	2
256	192	262	203	215	274	296	266	205	219	314	217	256	231	242	223	227	243	246	249	302

hariaensis (Plate 1, Figs. 7, 8) to the last appearance of *G. gansseri* (66.83–65.45 Ma) and spans the nannofossil *Micula murus* zone (Figs. 4, 5). At Mishor Rotem, the lower 2.2 m of the section analyzed mark zone CF3 as indicated by the co-occurrence of *Gansserina gansseri* and *P. hariaensis* (Fig. 6). Among small planktic foraminifera (63–150 μm), zone CF3 is dominated by *Heterohelix navarroensis* and *H. globulosa,* and one peak of *Guembelitria cretacea* (Fig. 7, Plate 1), whereas the larger species group (>150 μm) is dominated by *Heterohelix globulosa* (see also Abramovich and others, 1998).

Zone CF2. Zone CF2 defines the interval from the last appearance of *Gansserina gansseri* to the first appearance of *Plummerita hantkeninoides* (65.45–65.3 Ma, Fig. 4, Plate 2, Figs. 4–6) and corresponds to the lower part of the *Micula prinsii* zone (Fig. 5). At Mishor Rotem zone CF2 spans the interval from 2.2 m to 4.5 m, just below the first red layer (RL-1, Fig. 6). An undulating erosional surface marks the CF2/CF1 boundary. The smaller size fraction in CF2 is dominated by *H. globulosa* and *H. navarroensis,* though the latter decreases in the upper part of the zone, whereas a *Guembelitria cretacea* peak and corresponding decrease in *H. globulosa* marks the lower part of CF2 (Fig. 7). *Heterohelix globulosa* also dominates the larger size fraction, but decreases in the uppermost meter (Fig. 8).

Zone CF1. Zone CF1 defines the total range of *Plummerita hantkeninoides* (Plate 2, Figs. 4–6), which spans the last 300,000 kyr of the Maastrichtian (Pardo and others,

TABLE 2A. Mishor Rotem, Negev, Israel. relative percent abundance of planktic foraminifera in the upper Maastrichtian (> 150μ).

Biozone	Plummerita hantkeninoides CF1													
Sample number	7	8	9	10	11	12	13	14	16	18	19	20	21	21a
Sample depth (m)	7.00	6.90	6.80	6.70	6.60	6.50	6.40	6.30	6.20	6.10	6.05	6.00	5.98	5.97
Guembelitria cretacea	0	0	0	0	0	0	0	0	0	0	0	x	0	0
Globigerinelloides aspera	12	13	14	5	7	11	12	12	15	x	7	x	2	1
G. yaucoensis														
G. rosebudensis	3	x		1			1		1		1			
Globotruncanella minuta			1	x						x				
G. petalloidea	x	8	3	5	2	1	2	3	x	x	2	1	2	x
G. subcarinatus	1		x		x		1		2		2			x
Abathomphalus mayaroensis	x	x	x	x	x	x	x							
Globotruncana aegyptiaca		x	x	x	1	x	x	x	1	x			x	x
G. arca														
G. duwi					x	x	x	x	x	x				
G. dupeublei														x
G. esnehensis			x				x				x	x	x	x
G. insignis														
G. rosetta	x			x	x		x	x						x
Globotruncanita conica	x	x	x	x	x	x	x	x	x		x		x	x
G. pettersi														x
G. stuarti				x			1	x						x
Hedbergella holmdelensis														
H. monmouthensis														
Plummerita hantkeninoides	2	2	x	3	1	1	2	2	2	4	2	6	4	2
Rugoglobigerina hexacamerata														
R. macrocephala	5	6	12	10	9	4	4	3	4	7	5	5	5	9
R. pennyi												x		
R. reicheli	x			x				x	x	2		x	x	1
R. rugosa	7	6	5	6	11	2	2	3	2	3	2	7	3	7
R. scotti	x	x	3	2	x	1	1		x	2	1	2	3	1
Heterohelix globulosa	32	18	14	19	11	19	18	13	13	8	20	16	14	21
H. globulosa B	6	7	7	9	7	10	x	x	5	10	9	6	5	9
H. dentata	0	4	3	2	5	4	9	9	8	5	x	8	4	0
H. glabrans	1	1	0	0		0	2	0	2		0	0	1	0
H. labellosa	x	x	3	2	3	3	1		4	3	2	3	3	4
H. moremani		6				x	x				2	2		
H. navarroensis	5	0	2	5	2	x	4	1	5	4	3	2	4	0
H. planata	3	2	1	4	2	0	2	6	1	1	1	5	2	3
H. pulchra		x							x		x			
H. punctulata	1	3	4	2	x	2	3	9	3	x	x	x	5	4
Pseudoguembelina hariaensis	1	x	2	1	8	2			x	1	x	3	3	5
P. costulata	5	6	6	4	5	12	3	10	6	15	6	7	7	5
P. costellifera		3	3	8	1	1	1	x	4	3	3	x	4	2
P. kempensis	1	x		x	x	0	1	1	0	1	1	0	0	x
P. palpebra	1	4	x	2	3	0	5	7	4	4	5	2	1	3
Pseudotextularia elegans	5	2	4	1	8	14	13	11	9	14	16	9	10	10
P. nuttalli	x	1	1	2		x	1	1	x	2	1	x	2	1
Planoglobulina carseyae	7	5	6	5	9	9	7	7	3	5	5	10	13	7
P. brazoensis		x	x		x	x	x	x	x	x		x		x
P. multicamerata						x								
Racemiguembelina intermedia						x				x				
Juveniles no ID		x			x		x	x	x		2	1	x	x
Total counted	353	334	292	310	345	278	302	295	377	203	300	320	275	333

x = rare in > 150 μm size fraction, 0 = present in <150 μm size fraction.

1996; Li and Keller, 1998a, b) and corresponds to the upper part of the *Micula prinsii* zone (Fig. 5). At Mishor Rotem, this zone ranges from the base of RL-1 to the undulating erosional surface that marks the top of the last resistant chalk layer and underlies the K/T boundary (Figs. 2, 6). This undulating surface indicates erosion of part of the uppermost Maastrichtian prior to deposition of the K/T boundary clay. The smaller size fraction is dominated by *H. globulosa* and *H. narvarroensis* with a peak of *G. cretacea* in the lower half (between RL-2 and RL-3), whereas *G. aspera* is common in the upper part (Fig. 7). In the larger size fraction, *H. globulosa* is less abundant than in CF-2 and CF-3, but there is increased abundance of *Pseudotextularia elegans, Pseudoguembelina costulata, H. dentata* and in the upper part, *G. aspera* (Fig. 8, Plate 1).

Zone P0. Zone P0 marks the K/T boundary and is defined as the interval between the extinction of Cretaceous tropical and subtropical planktic foraminifera and the first appearance of *Parvularugoglobigerina eugubina* and/or *P. longiapertura* (Fig. 4, Keller and others, 1995). Lithologically, zone P0 is marked by a dark clay layer with a thin red clay at the base. At Mishor Rotem, the K/T boundary is not easily identified in the field because there is no dark clay layer as a result of erosion, as also observed in many other

TABLE 2A. Extended.

Plummerita hantkeninoides CF1																			CF3		
21c 5.95	22 5.91	23 5.85	24 5.75	25 5.65	26 5.55	27 5.45	28 5.35	29 5.25	30 5.15	31 5.05	32 4.95	33 4.85	34 4.75	35 4.71	36 4.65	37 4.60	38 4.55	39 4.50	40 4.40	41 4.30	42 4.10
1	0	0	x	0	0	0	0	0	0	0	0	0	0	x	1	1		0	1	0	0
x	2	1	x	0	1	0	2	x	1	3	1	1	2	2	6	4		2	1	2	2
						x							0			x					0
													0								
	0																				
1	1		1	1	x		1	x	x		1		2					x		0	1
1	1		2				1		1	2				x	2	1		x	1		0
x	x	x	x	1	x	x	x	1	1	1	x	x	x		x	x		x		1	1
		x				x		1				x	x							x	
								x	x	x			x				d				
										x							i				x
	x		x	x	x	x		x	x	x			x			x	s	x		x	
	x			x													s	x			
				x		x	x	x	x	x		x					o				
	x	x	1			x	x										l			x	1
							x								x		u				
x	x		x		x		x		x	x			x				t	x		x	x
													0		1		i	x		x	x
		x										0	0		1	x	o	0			0
2	3	4	1	2	1	2	3	4	2	3	3		2	2	1		n	x			
						x					x	x	x								
11	10	7	9	7	5	5	6	9	8	6	7	6	8	4	3	4		8	2	6	13
	x								x	x	x										1
x		1	1		1	x	2	1		2	2	1	2		x			6	2	0	2
4	5	4	3	6	3	4	2	2	x	1	3	2	3	x	x	1		4	2	2	**6**
3	2	x	1	x	1	1	1	1	4	2	x	1	3	x	1	2		2	1	2	**4**
27	25	22	21	26	28	27	30	8	20	23	16	19	22	21	19	11		11	11	5	**11**
x	3	8		4	3	3	7	4	8	5	12	8	6	11	9	19		3	12	21	**24**
1	3	2	2	7	7	8	7	6	7	9	5	4	5	2	5	x		8	7	9	**4**
x		0	0	0	1	0	0	1	x	1	2	x	x	0	1	3		1	2	0	**1**
x	2	3	5	4	6	4	x	8	x	2	3	5	2		1			2	1	3	**x**
	x																				
4	0	0	x	0	0	3	4	3	4	x	3	4	4	5	11	8		x	3	x	**2**
x	2	8	3	3	x	1	2	4	1	3	2	5	3	7	x	1		6	6	2	
			x			x				x		x		x	x	2					
5	4	3	10	8	2	6	2	5	4	3	4	5	2	4	3	6		7	4	5	**2**
4	1	2	1	3	1	x	4	4	2	2	3	5	2	1	2	1		2	2	3	
8	11	5	5	3	7	7	3	8	4	4	6	6	4	11	5	10		7	10	9	**3**
4	1	2	4	2	4	1	8	7	5	5	1	3	6	8	7	11		4	12	6	**4**
1	x	x	1		x	x	0	1	x	x	x	x	0	2	1	2		2	1	4	**x**
3	5	6	4	4	7	2	3	4	5	5	4	2	5	3	1	x		4	4	5	**5**
6	9	6	9	8	7	12	6	7	12	10	9	11	6	11	8	8		10	11	6	**4**
1	2	2	2	2	1	2	2		1		3	2	1		4			2	x	2	**1**
11	6	9	10	5	7	7	2	6	6	5	8	5	7	4	4	3		6	1	6	**5**
	x	x	x	x	x	1		x	x			1	x	x		x				x	**x**
															x					x	
		x		x	1	1	x	1	x		x	x	x	1				x	x		**x**
236	375	339	346	304	332	332	301	273	249	308	312	322	265	190	252	228		321	148	285	**280**

sections (Magaritz and others, 1985; Rosenfeld and others, 1989; Keller and Benjamini, 1991). However, a thin red layer (2–4 mm) with spherules and an Ir anomaly (see Lithology section) is discontinuously present (Fig. 2). The first Danian species of zone Pla appear in the marl immediately above the red layer. Most Cretaceous species are present in the basal Danian sediments above the K/T boundary red layer due to reworking (Fig. 7), as also observed in many other section in southern Israel (Keller and Benjamini, 1991).

Zone Pla. This zone is defined by the range of *Parvularugoglobigerina eugubina* and/or *P. longiapertura.* Zone Pla can be subdivided based on the first appearance of *Parasubbotina pseudobulloides* and *Subbotina triloculinoides* (Fig. 5). At Mishor Rotem, the presence of a diverse early Danian assemblage, including the above index species, indicates that the upper part of zone Pla, or subzone Pla(2), directly overlies the boundary red clay. This is also suggested by the presence of early Danian species in the 63–105 μm size fraction, which generally do not occur until subzone Pla(2) (Keller and others, 2002). The early Danian subzone Pla(1) is thus absent due to a short hiatus as suggested by the abundance of reworked Cretaceous species near the base of subzone Pla(2) (Figs. 7). An early Danian zone Pla hiatus has been observed in all other studied sections of the Negev (Keller and Benjamini, 1991), and in

TABLE 2B. Mishor Rotem, Negev, Israel. Relative percent abundance of planktic foraminifera in the upper Maastrichtian (>150 μ).

	CF3																								
Biozone Sample number Sample depth (m)	43 4.1	44 4.0	45 3.9	46 3.8	47 3.7	48 3.6	49 3.5	50 3.4	51 3.2	52 3.1	54 3.0	56 2.8	58 2.6	60 2.4	62 2.2	64 2.0	66 1.8	68 1.6	70 1.4	72 1.2	74 1.0	76 0.8	78 0.4	80 0.2
Guembelitria cretacea	0	0	0	0	0	0	0	0	0	0	0	0	0	0	0	0	0	0	0	0	0	0	0	0	0
Globigerinelloides aspera	2	2	1	4	3	1	0	5	4	3	8	6	3	1	1	3	1	5	6	3	5	2	3	7	
G. yaucoensis	0	0	0		x			0												0	0	1	0	0	
G. rosebudensis				1	0			0	0		x	1	0	0	1	1	1	1	2	x		0	1	x	
Globotruncanella minuta							1							1	3	2	0	7	3	1	5	4	7	6	
G. petalloidea	3	2	3	2	1	1	1	4	4	4	4	2	1		2	1	x	5	5	2	3	6	2	x	
G. subcarinatus	2	4	0	1	x	1	2	2	1	1	2	0	1	2	2	2	2	2	0	1	1	x	5	x	
Archeoglobigerina cretacea																				x				x	
A. blowi																			x	x		1	1		
Abathomphalus mayaroensis										x		x								x					
Gansserina gansseri	x														1					x	1	1	1	x	
Globotruncana aegyptiaca		x	x	x	1		x					1		x	x					3	x	1	1	x	
G. arca																					x				
G. duwi					x																				
G. dupeublei																			x						
G. esnehensis	1				x	x	x	x	x	x	x	x	x	x	x	1	x		x	x	x	x	x	x	
G. insignis		x		x	x			x	x	x				x	x		x				x	x	x	x	
G. rosetta					x							x	x												
Globotruncanita conica	x	x	x		x	x	x		x	x	x	x	x	x	x	1	x		1	x	x	x	x	x	
G. pettersi	x	x	x	x	x	x			x		x			x	x				x	1	x		x	x	
G. stuarti				x						x												x			
Rosita contusa																				x					
Hedbergella holmdelensis		0		x	x	0		x		0	x		1			x				0		1	x	0	
H. monmouthensis	0	0				0	0	0		0	0	0	0	1		0	0	0	0	0	0	0	x	0	
Plummerita hantkeninoides																									
Rugoglobigerina hexacamerata																									
R. macrocephala	10	6	10	5	14	10	6	9	10	6	3	10	12	6	9	12	12	4	8	14	13	4	7	x	
R. pennyi	x					x			x																
R. reicheli	x	3																							
R. rugosa	3	3	2	3	6	5	4	6	4	1	3	4	3	5	5	7	7	1	1	6	8	6	2	12	
R. scotti	4	0	0	1	5	1	x	3	6	3	1	3	6	4	2	2	8	3	1	3	3	2	6	x	
Heterohelix globulosa	9	10	6	5	11	13	12	14	8	17	20	10	24	14	8	11	9	6	13	11	14	15	18	10	
H. globulosa B	15	26	44	25	23	46	41	21	30	17	21	20	19	21	15	20	17	22	25	15	10	18	14	13	
H. carinata												4													
H. dentata	3	5	1	1	x	0	0	1	4	x	9		4	3	7	8	6	13	8	4	1	x	x	x	
H. glabrans	2	2	1	3	1	x	2	1	0	0	3	2	0	0	0	x	0	2	3		1	x	2	1	
H. labellosa	3		5	3	1		5	5	3	2	2	4	4	1	2	2	1	3	1	1	2	x		1	
H. moremani	x		2	3	1	x		1	1	3	3	3	2	9	9	7			4	6	7	8	6	9	
H. navarroensis	3	3	0	7	0	2	x	4	1	x	3	0	0	3	0	0	6	5	1	0	1	4	0	x	
H. planata		2				1	1	2		5	1	1	2	2		4				x					
H. pulchra																	x								
H. punctulata	4	2	4	1	3	9	2	4	2	8	2	6	1	2	4	1	4	2	3	4	4	2	1	5	
Pseudoguembelina hariaensis	5	2		x	2	x	x		2	4	1	2		2	1	2	3	2	3	4	1	2	2	3	
P. costulata	4	7	3	5	3	x	2	7	3	3	4	2	3	5	5	4	7	4	5	1	2	8	10	5	
P. costellifera	6	5	2	4	5	x	7	x	2	4	4	3	2	3	x			x								

TABLE 2B. Continued.

Biozone	CF3																							
Sample number	43	44	45	46	47	48	49	50	51	52	54	56	58	60	62	64	66	68	70	72	74	76	78	80
Sample depth (m)	4.1	4.0	3.9	3.8	3.7	3.6	3.5	3.4	3.2	3.1	3.0	2.8	2.6	2.4	2.2	2.0	1.8	1.6	1.4	1.2	1.0	0.8	0.4	0.2
P. kempensis	0	x	0	x		0	0		x		x					1								
P. palpebra	4	2	3	2	3	2	2	2	2	5	1	3	3	1	2	2	3	2		4	2	2	2	4
Pseudotextularia elegans	5	4	5	10	5	1	3	3	4	4	1	3	3	5	5	2	2	3	1	3	5	1	1	5
P. nuttalli	2	2	2	1	1	1	2	3	5	3	x	3	4	3	4	1	4	3	1	5	7	4	4	2
Planoglobulina carseyae	6	4	4	9	6	4	3	3	2	4	1	4	2	2	7	1	4	3	2	4	1	3	2	3
P. brazoensis		x	x	x	x	x		x	x		x		x		2	x			x		x		x	x
P. multicamerata	x									x														
Racemiguembelina intermedia																								
Juveniles no ID	x	x			x		x	1	x				x	x			x	x	1	1	1	1		
Total counted	314	272	283	254	321	288	330	289	316	300	345	271	252	278	282	293	255	293	258	263	243	278	263	320

x = rare in >150 µm size fraction, 0 = present in < 150 µm size fraction.

many early Danian sections worldwide (MacLeod and Keller, 1991), and may thus represent a regional, if not global, sea level change. The overlying subzone Pla(2) spans 45 cm of shaly marl that forms the base of the Taqiye Formation (Fig. 2). Subzone Pla(2) is dominated by *Parvularugoglobigerina longiapertura* and increasing abundances of *P. extensa, S. triloculinoides, P. pseudobulloides* and *C. midwayensis* (Fig. 7).

FORAMINIFERAL POPULATIONS

Species Richness Patterns

Species diversity is the total number of species in an assemblage, whereas species richness reflects the actual number of species present at a given time and is therefore a measure of environmental variability (e.g., climate, seasonality, nutrient fluctuations), but may be influenced by fossil preservation (e.g., dissolution, breakage of shells). Species richness may be significantly lower than species diversity as a result of sample preservation, climate variations and/or local environmental conditions. For example, in the absence of preservational bias at El Kef, species diversity at the end of the Maastrichtian is estimated between 55–65 species based on extensive surveys conducted as part of a blind test to find every possible species (Olsson, 1997; Orue-etxebarria, 1997; Masters, 1997; Keller and others, 1995, 2002b), but species richness is only between 45–55 species, Li and Keller, 1998c). This means that up to one third of the species are absent or too rare to be detected by normal statistical analysis in most sample intervals. These rare species are ecologic specialists, driven to near-extinction as a result of changing environmental conditions and elimination of their ecological niches.

Species richness at Mishor Rotem is unusually low during the late Maastrichtian and narrowly fluctuates around 30 species, except for the lower part of the section where 33–35 species are present and across the lowermost red layer (RL-1) where it drops to 21–22 species (Figs. 6, 9). Even lower species richness was observed at Qreiya in central Egypt with 22–30 species in zones CF3-2, with a brief interval of 32–33 species in CF1 (Fig. 9, Keller, 2002). Sediment deposition at these localities occurred at outer neritic-upper bathyal and middle-outer neritic depths, respectively. Comparable depth localities in Tunisia, Spain, and Mexico average 45–55 species (Lopez and Keller, 1996; Pardo and others, 1996; Abramovich and Keller, 2002). Fossil preservation at Qreiya or Mishor Rotem is relatively good and does not account for the low species richness, which appears to be regional throughout Israel and Egypt (Keller and Benjamini, 1991; Abramovich and others, 1998; Keller, 2002). To understand these unusually impoverished species assemblages, it is helpful to examine species richness patterns across the continental shelf in Tunisia.

Species richness and diversity tend to be highest in outer shelf-upper slope environments (250–500 m) and progressively decrease in shallower waters across the continental shelf. This can be demonstrated in Tunisia, where preservational bias is not a major factor in generally well preserved foraminiferal assemblages. In the upper Maastrichtian zones CF1 to CF3, species richness varies between 42–54 species at the outer shelf-upper slope section at El Kef

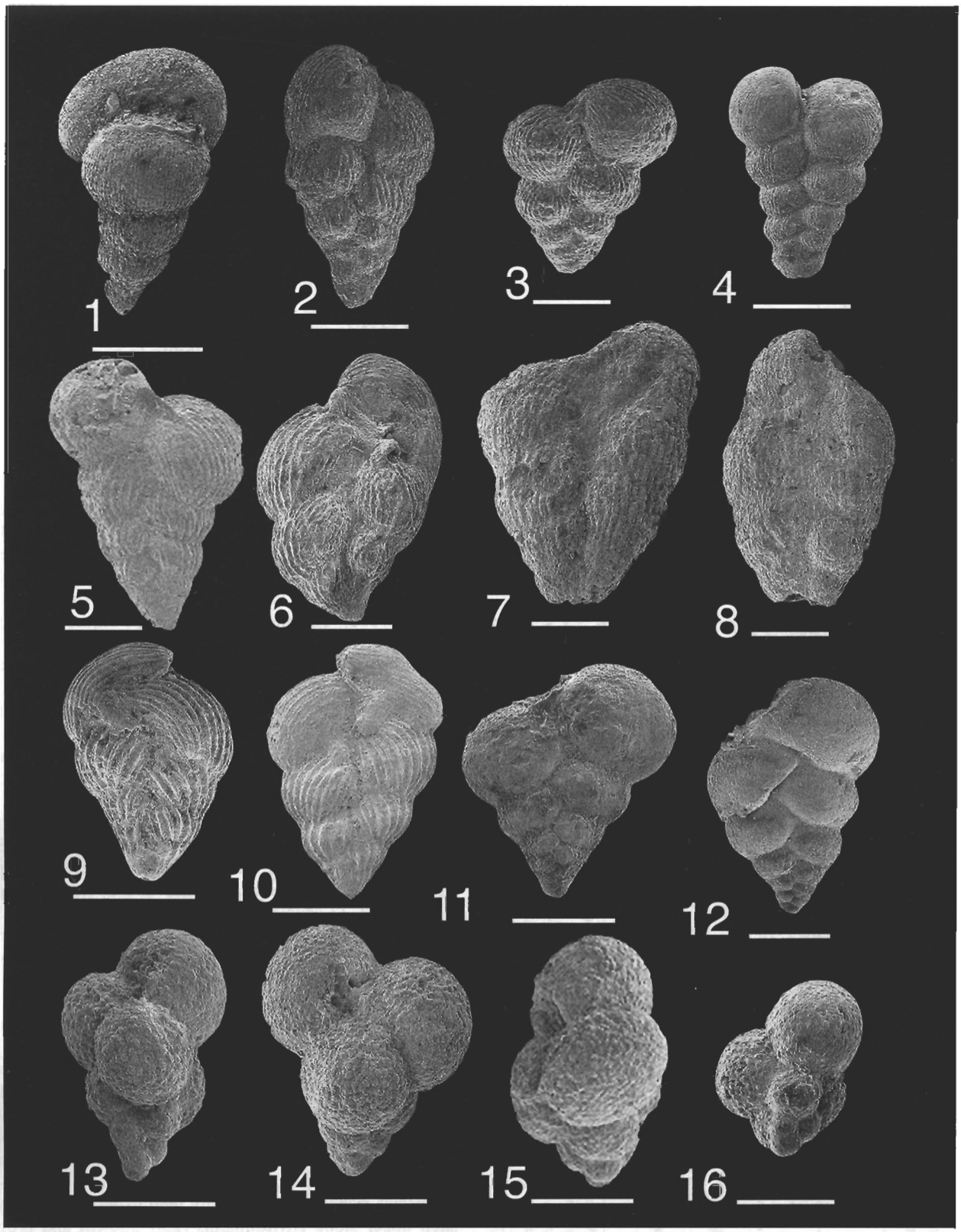

PLATE 1

All specimens from the upper Maastrichtian *P. hantkeninoides* zone of the Mishor Rotem section, Israel. Scale bar = 100 μm for Figures 1–12 and 50 μm for Figures 13–16.

1. *Pseudotextularia elegans,* 2. *Heterohelix dentata,* 3. *H. globulosa,* 4. *H. navarroensis,* 5. *Pseudoguembelina costellifera,* 6. *P. palpebra,* 7, 8. *Plummerita hariaensis,* 9, 10. *Pseudoguembelina costulata,* 11, 12. *Laeterohelix glabrans,* 13–15. *Guembelitria cretacea,* 16. *G. trifolia.*

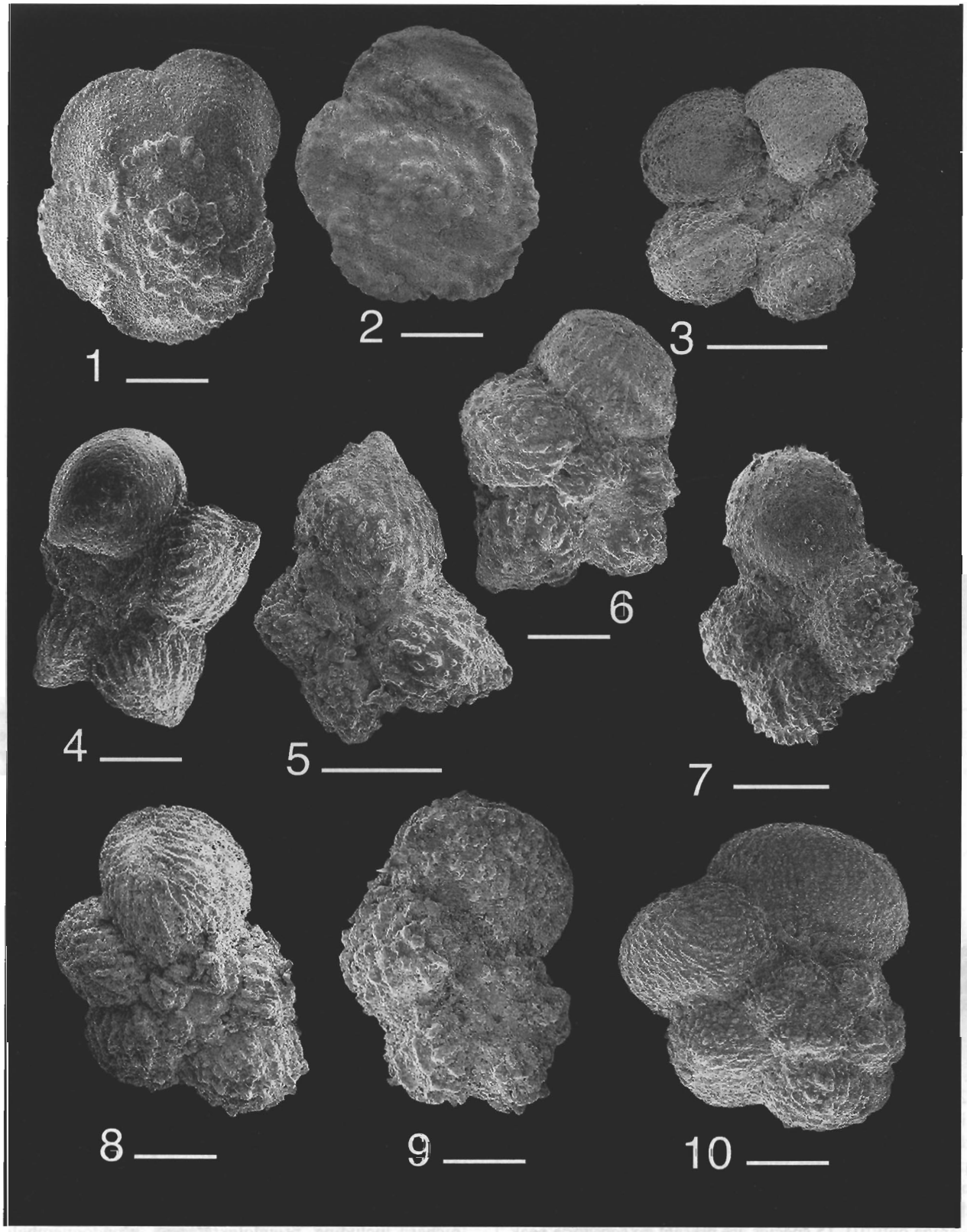

PLATE 2

All specimens from the upper Maastrichtian *P. hantkeninoides* zone of the Mishor Rotem section, Israel. Scale bar = 100 μm.
1. *Globotruncana esnehensis,* 2. *Abathomphalus mayaroensis,* 3. *Globotruncanella petaloidea,* 4–6. *Plummerita hantkeninoides,* 7. *Globigerinelloides subcarinatus,* 8. *Rugoglobigerina rugosa,* 9, 10. *R. scotti.*

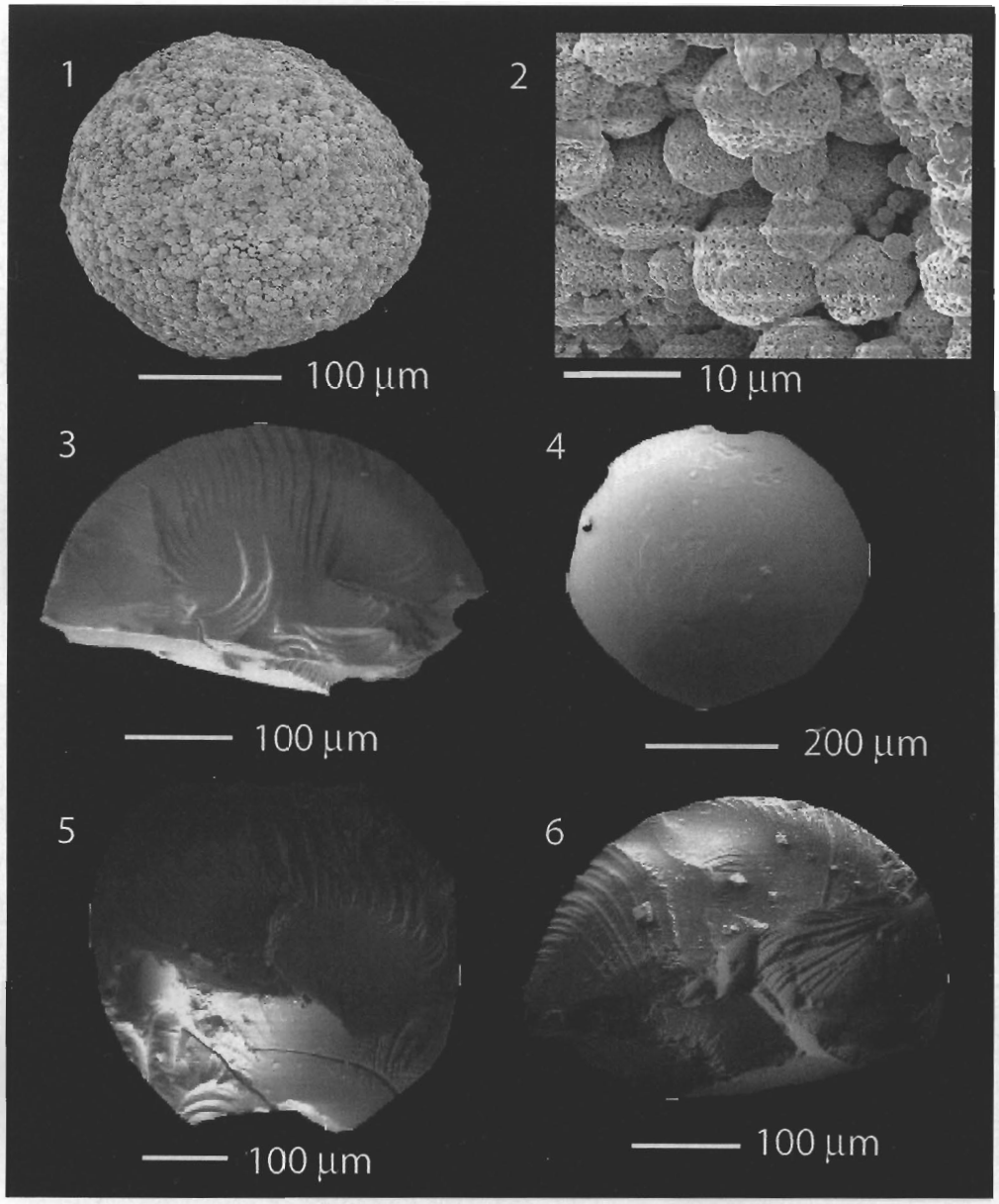

FIGURE 3. Spherules from the Mishor Rotem red layers RL-1 to RL-4. 1–2, Fe-rich spherule and surface detail from the K/T red layer (RL-4) and Ir anomaly. 3–6, Translucent, yellow amber spherules from the upper Maastrichtian red marl layers showing conchoidal fractures and surface details. The chemical composition is almost pure carbon (~90–95%). These are amber spherules derived from the late Cretaceous forests of Jordan and Syria (Bandel and others, 1997).

(Fig. 10, Keller, 1988; Li and Keller, 1998c; Keller and others, 2002b). At the shallower middle neritic locality of Elles, species richness is consistently lower, but shows similar trends (Abramovich and Keller, 2002), though different sample resolutions at the two localities prevent precise correlation. The lowest species richness is found at the inner-middle neritic locality of Seldja in southern Tunisia where on average only 10–15 species are present, except for a peak of 24 species marking an incursion of open marine species associated with a sea level rise (Keller and others, 1998).

Species richness is directly related to niche availability, which is related to water depth and watermass stratification. In shallow inner neritic environments species richness is lowest because ecological niches are largely restricted to the surface mixed layer (~50 m) of the upper photic zone (e.g., Leckie, 1987; Keller and others, 1998). This environment is primarily populated by ecological opportunists (*Guembelitria*) and generalists (small heterohelicids, hedbergellids, globigerinellids, and rugoglobigerinids, Keller and others, 2002b). In deeper middle neritic environments (~100–200 m), more specialized species occupy various ecological niches, including pseudotextularids, pseudoguembelinids, racemiguembelinids and some keeled globotruncanids. Ecologic niche availability is at a maximum in deeper outer neritic to upper slope environments with well stratified watermasses, and so is species richness with the addition of highly specialized, large and ornate species living at or below thermocline depths (e.g., globotruncanids, gublerinids,

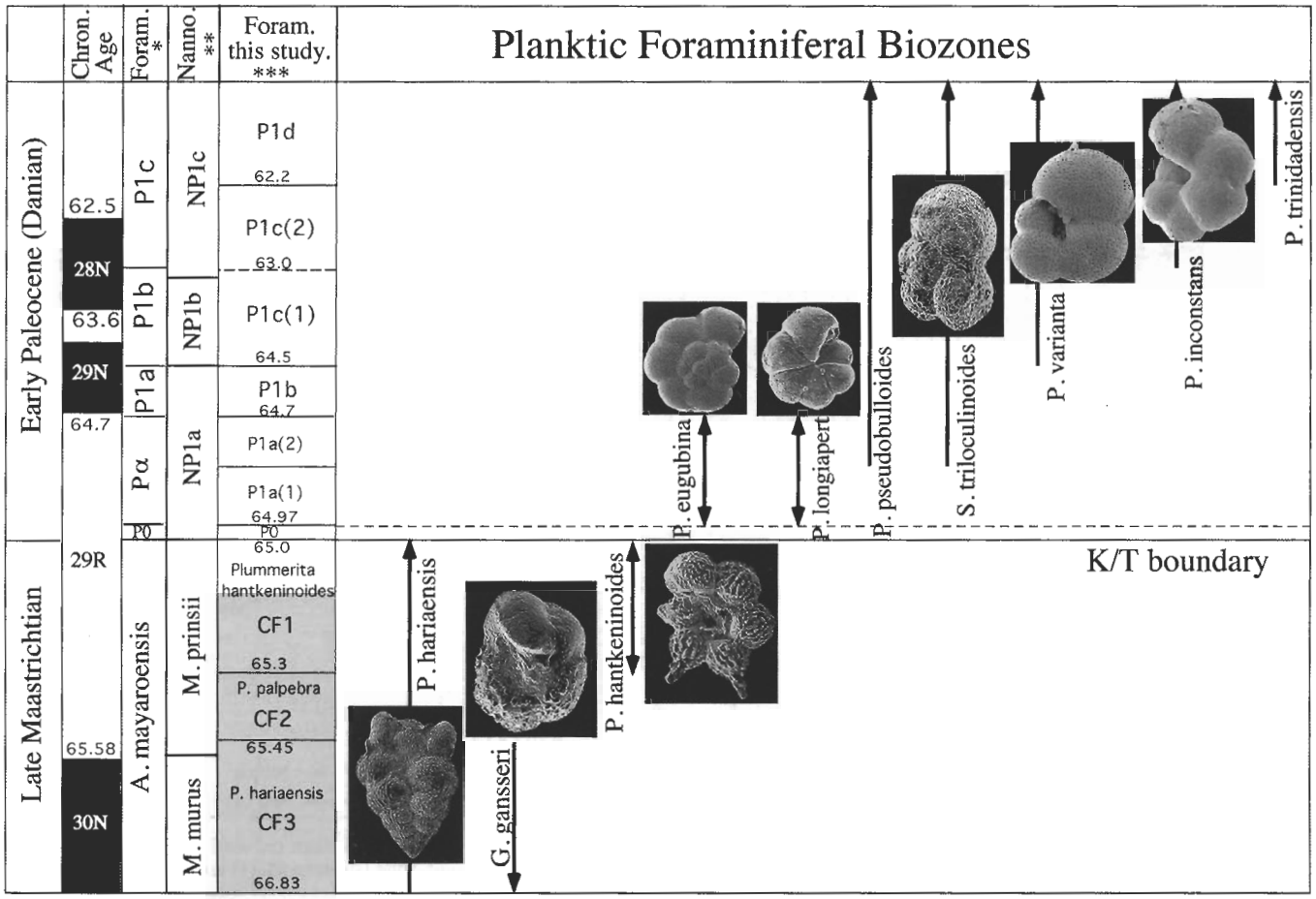

FIGURE 4. High-resolution planktic foraminiferal biozonation for the late Maastrichtian (Li and Keller, 1998b) and early Danian (Keller and others, 1995). Note that this biozonation significantly refines the resolution for the upper Maastrichtian by replacing the upper *Abathomphalus mayaroensis* zone by three biozones and by subdividing the *Parvularugoglobigerina eugubina* (Pla) zone into two subzones based on the first appearances of *Parasubbotina pseudobulloides* and *Subbotina triloculinoides.*

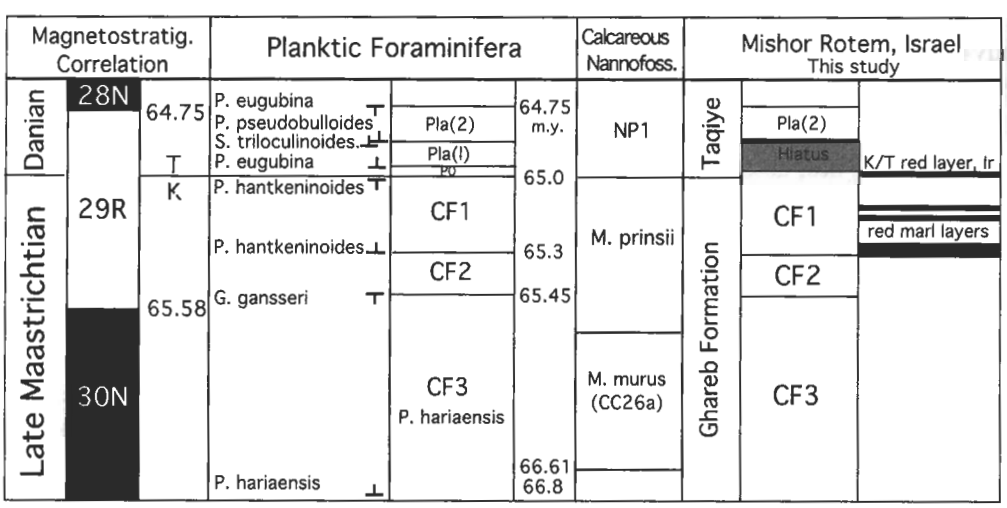

FIGURE 5. Biostratigraphy of the Mishor Rotem section based on planktic foraminifera and calcareous nannofossils tied to the planktic foraminiferal biozonation of Li and Keller (1998b) and Keller and others (1995). Note the section has an early Danian hiatus, and the three red layers are present in the lower part of zone CF1.

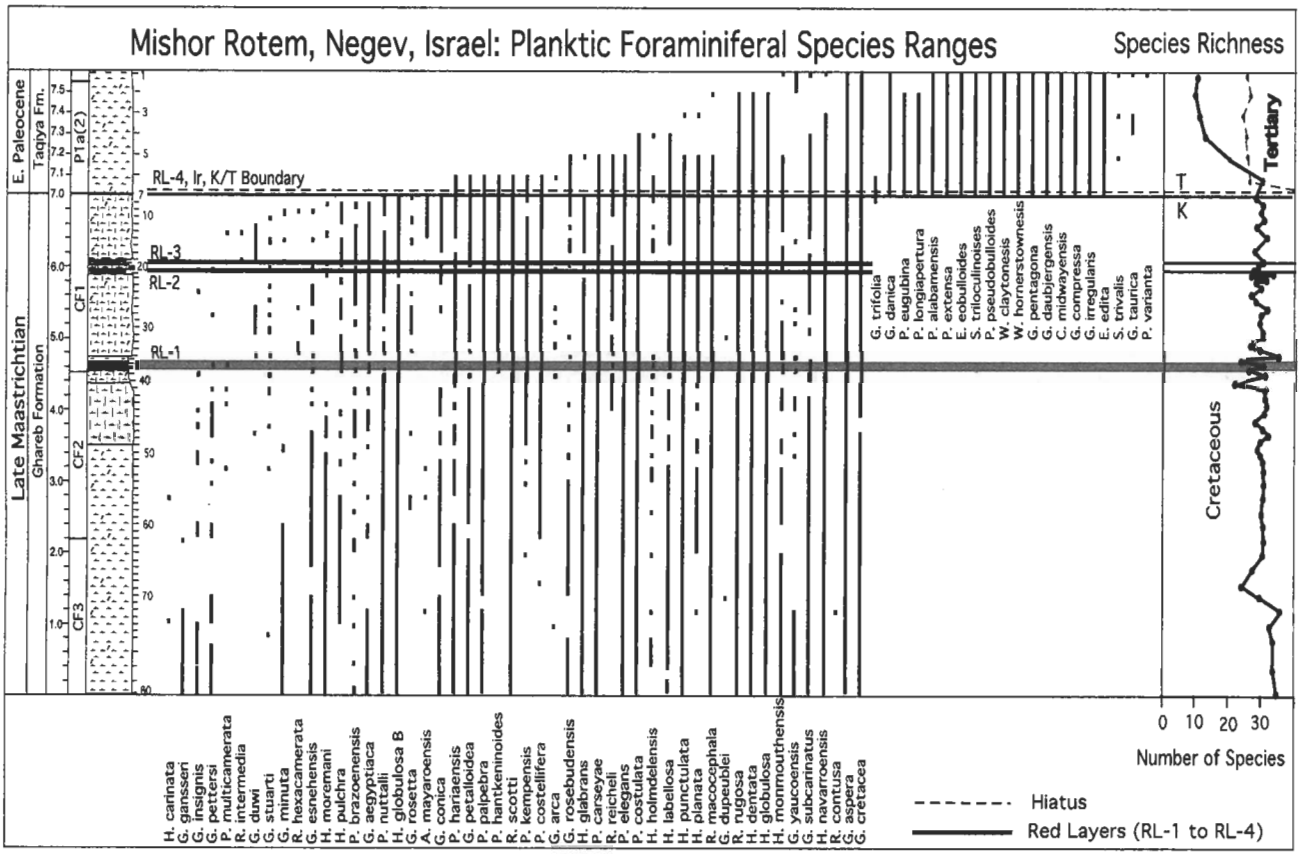

FIGURE 6. Planktic foraminiferal species ranges and species richness at Mishor Rotem, Israel. Grey lines mark red marl layers (RL-1 to RL-4); dashed line marks hiatus at the K/T boundary where zones P0 and the lower part of the *P. eugubina* zone (subzone Pla(1) are missing. Note species richness is unusually low at 28–30 species and nearly one third below normal Tethyan assemblages. Most Cretaceous species in the early Danian are reworked.

planoglobulinids). The progressive increase in species richness across the continental shelf is thus directly related to increasing water depth and water mass stratification that provide specialized niche habitats related to variations in temperature, nutrients, oxygen and salinity. Intraspecific variations in stable isotope signals of species confirm these trends (D'Hondt and Arthur, 1995; Abramovich and others, 2003).

The significantly lower (~30%) species richness in central Egypt and southern Israel, compared with Tunisia, appears to be the result of special environmental conditions, as indicated by dominance of ecological opportunists and generalists, and the absence or near absence of most deeper water dwellers (e.g., globotruncanids) despite water depths where these species normally thrive (Figs. 7, 8, Keller, 2002). Clues to the nature of these high stress conditions can be gained from presence/absence data and the relative abundances of ecological generalists, specialists and opportunists.

PALEOENVIRONMENT OF PLANKTIC FORAMINIFERA

Ecological Generalists

More than half of the late Maastrichtian assemblages in the small (63–150 μm) size fraction and almost half in the larger (>150 μm) size fraction are dominated by small biserial heterohelicids (*Heterohelix globulosa, H. dentata, H. navarroensis, H. labellosa, H. moremani*; Fig. 11, Plate 1). Heterohelicids are the garden weeds of the foraminiferal community. These biserial taxa are characterized by medium or small test sizes, simple morphologies, little surface ornamentation, and nearly global biogeographic range. They appear to have tolerated significant fluctuations in temperature and/or salinity, oxygen and nutrients and can therefore be considered ecological generalists. The isotopic compositions of these species indicate that they lived below the surface mixed layer and thrived at times of an expanded oxygen minimum zone (Boersma and Premoli Silva, 1989; Barrera and Keller, 1994; MacLeod and others, 2001; Abramovich and others, 2003), whereas their global biogeographic distribution suggests a tolerance for temperature changes (Nederbragt, 1998). *Heterohelix globulosa,* the most abundant of these species, tends to exhibit a preference for continental margins (Leckie, 1987; Keller, 1989; Malmgren, 1991). Late Maastrichtian heterohelicid dominance has been observed in sections throughout Israel, Egypt, Tunisia, Italy, Spain, Texas, Denmark and DSDP Site 525 (Keller, 1988, 1989, 2002; Nederbragt, 1991, 1998; Malmgren, 1991; Keller and others, 1995, 1993; Luciani, 1997, 2002; Abramovich and others, 1998; Li and Keller, 1998b; Abramovich and Keller, 2002). Dominance of these ecological generalists in southern Israel likely reflects an expanded oxygen minimum zone and generally dysaerobic conditions.

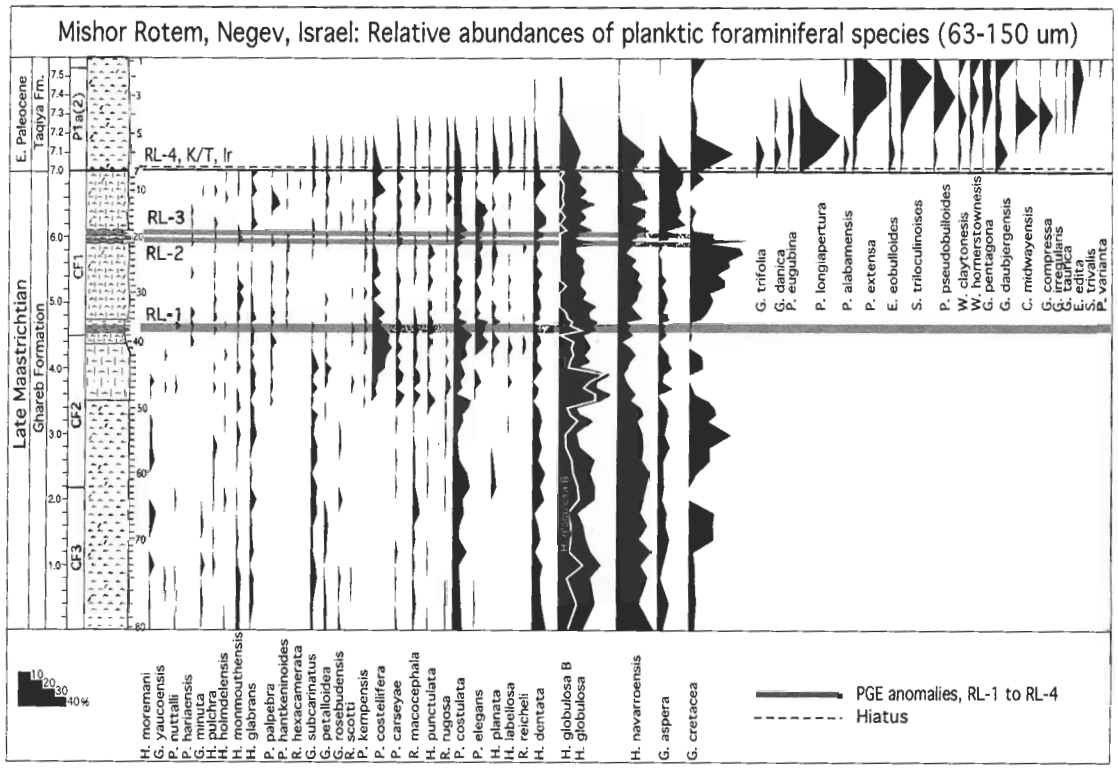

FIGURE 7. Relative abundance of planktic foraminifera in the 63–150 μm size fraction at Mishor Rotem, Israel. Note the low species diversity, dominance of low-oxygen-tolerant heterohelicids (*H. globulosa, H. navarroensis*), and blooms of the opportunist *Guembelitria* in the upper Maastrichtian. *Heterohelix globulosa* B is a large morphovariant of *H. globulosa.* Presence of common Cretaceous species in lower Danian sediments is due to reworking. Grey lines mark red marl layers, dashed line at K/T boundary marks hiatus.

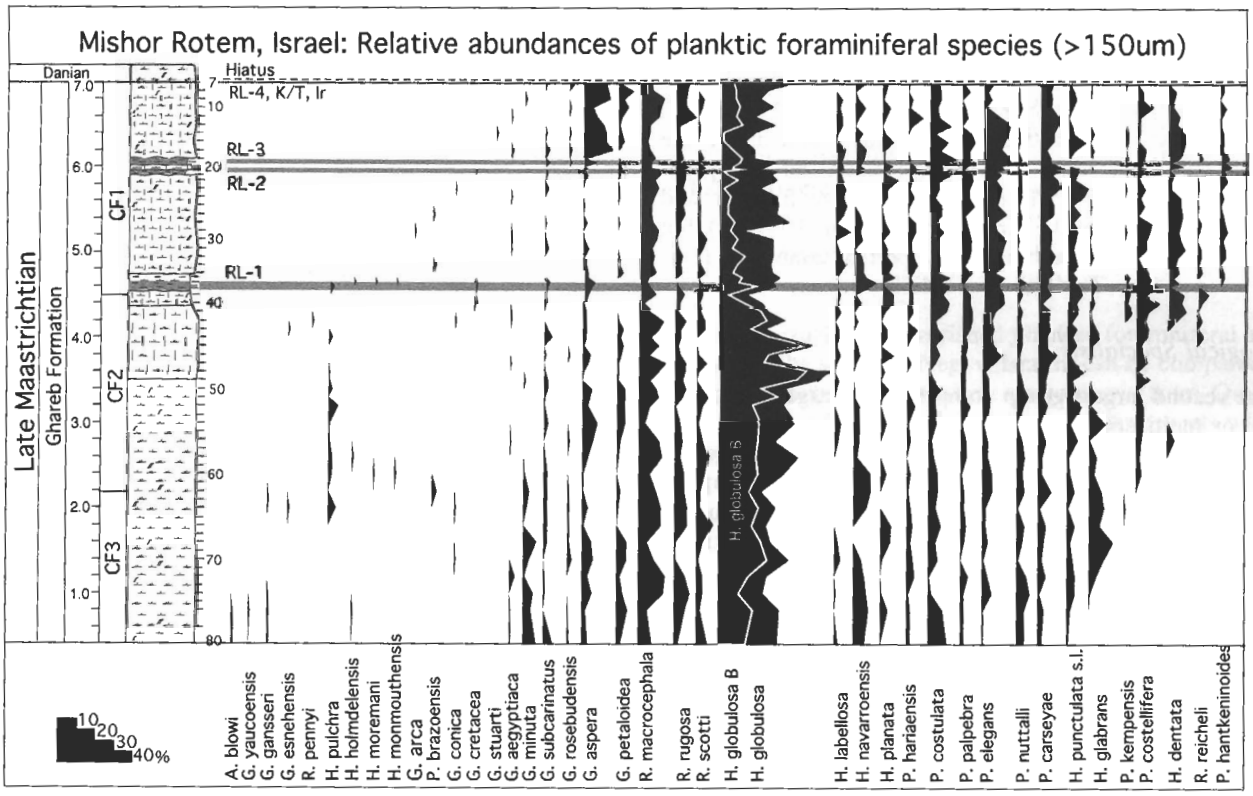

FIGURE 8. Relative abundance of planktic foraminifera in the >150 μm size fraction at Mishor Rotem, Israel during the late Maastrichtian. Note dominance of *H. globulosa* (including the large morphovariant *H. globulosa* B), common larger biserial taxa (*P. elegans, P. carseyae*), and rare sporadic occurrences of globotruncanids. Grey lines mark red marl layers, dashed line at K/T boundary marks hiatus.

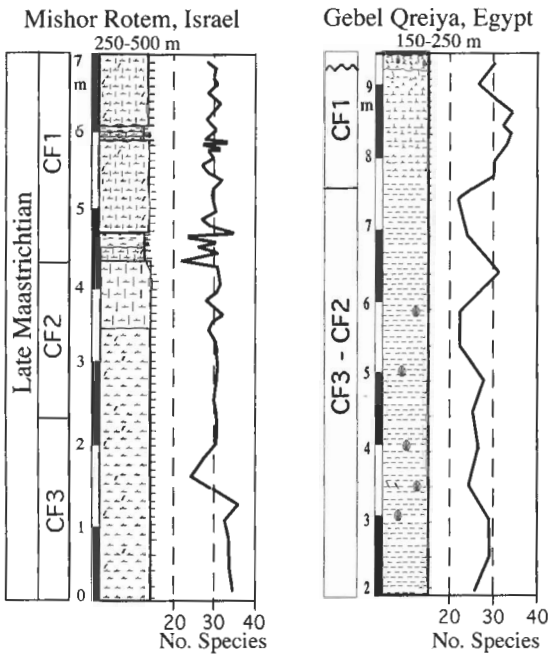

FIGURE 9. Planktic foraminiferal species richness at Mishor Rotem, Israel, and Gebel Qreiya, Egypt. Note late Maastrichtian species richness in both localities is unusually low (25–32 species) compared with normal Tethyan assemblages (45–50 species). At Qreiya, species richness is on average lower than in southern Israel. Low species richness reflects adverse environmental conditions for species habitats and life modes.

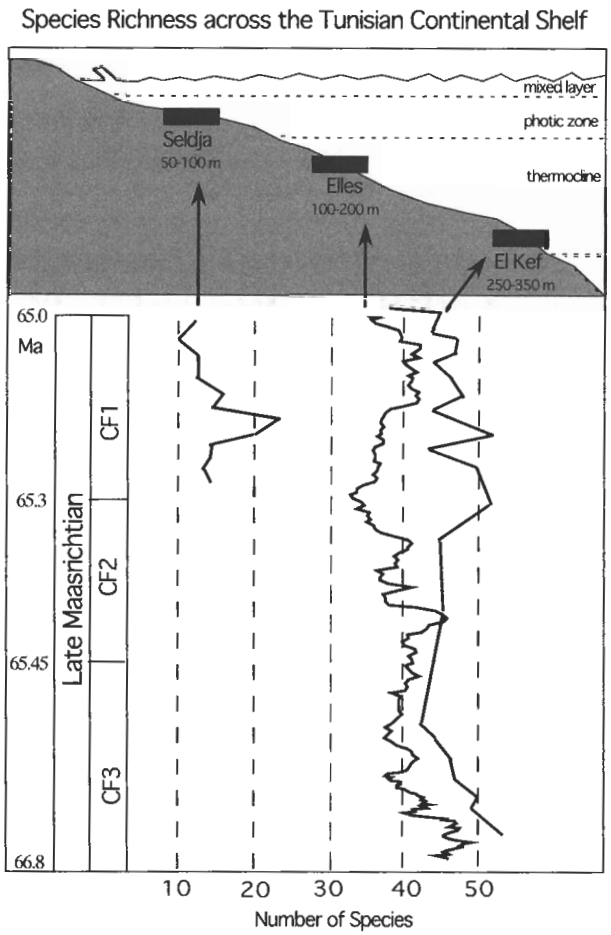

FIGURE 10. Planktic foraminiferal species richness across the Tunisian continental shelf-slope based on data from the inner shelf Seldja section (Keller and others, 1998), middle shelf Elles section (Abramovich and Keller, 2002), and outer shelf to upper slope El Kef section (Li and Keller, 1998c). Note that species richness increases with increasing depth across the shelf and is a function of available ecological niches and depth habitats.

Small planispiral and trochospiral species, including *Globigerinelloides aspera, G. yaucoensis, Hedbergella monmounthensis, H. holmdelensis, Rugoglobigerina rugosa* and *R. macrocephala,* constitute another group of ecological generalists with a widespread geographic distribution, but living largely in the photic zone (surface) and above the oxygen minimum zone. At Mishor Rotem, this group accounts for less than 15% in the smaller size fraction, and only slightly more in the larger size fraction (10–20%), but increases to 30% in the uppermost part of zone CF1 (Fig. 11).

Ecological Specialists

The second largest group comprises the large, ornate, biserial or multiserial species of the genera *Pseudoguembelina, Pseudotextularia, Planoglobulina* and *Racemiguembelina* (Fig. 11, Pl. 1). In the larger size fraction (>150 μm), this group averages 25% in zones CF2 and CF3, but increases to 40% in CF1 and decreases to 20% by K/T time. Species of this group have narrow tolerance limits and geographic ranges restricted to low and mid-latitudes. Stable isotopic ranking shows them to be surface dwellers. Other surface-dwelling ecological specialists (small trochospiral species) of the *Rugoblobigerina* group (*R. scotti, R. hexacmerata, Plummerita hantkeninoides,* Pl. 2) are rare, except during the warming in zone CF1, which reflects the global climate warming between 65.4–65.2Ma (Li and Keller, 1998a, b).

Most notably absent in upper Maastrichtian sediments of southern Israel is the second group of ecological specialists, the deeper dwelling (thermocline) globotruncanids with heavily calcified tests, keels and ridges. Globotruncanids are rare and only sporadically present at Mishor Rotem (Fig. 8). Although 11 species are recorded, their combined relative abundance rarely exceeds 1%. Similar rarity of this group has been recorded from other sections in southern Israel (Abramovich and others, 1998). The absence of globotruncanids in this outer shelf to upper bathyal depositional environment is likely related to an expanded oxygen minimum zone (suggested by abundant biserial species) and dysaerobic conditions into the thermocline layer, and hence the reduction of ecological niche space for this species group.

Ecological Opportunists

The most unusual aspect of the late Maastrichtian faunal assemblages at Mishor Rotem are three abundance peaks in *Guembelitria cretacea* (20–40%, >63 μm size fraction, Figs. 7, 12, Pl. 1, Figs. 13–16). Similar abundance peaks have been observed throughout southern Israel (Abramovich and others, 1998), and even higher abundances (70–90%) in central Egypt (Fig. 12). In Tunisia, correlative *Guembel-*

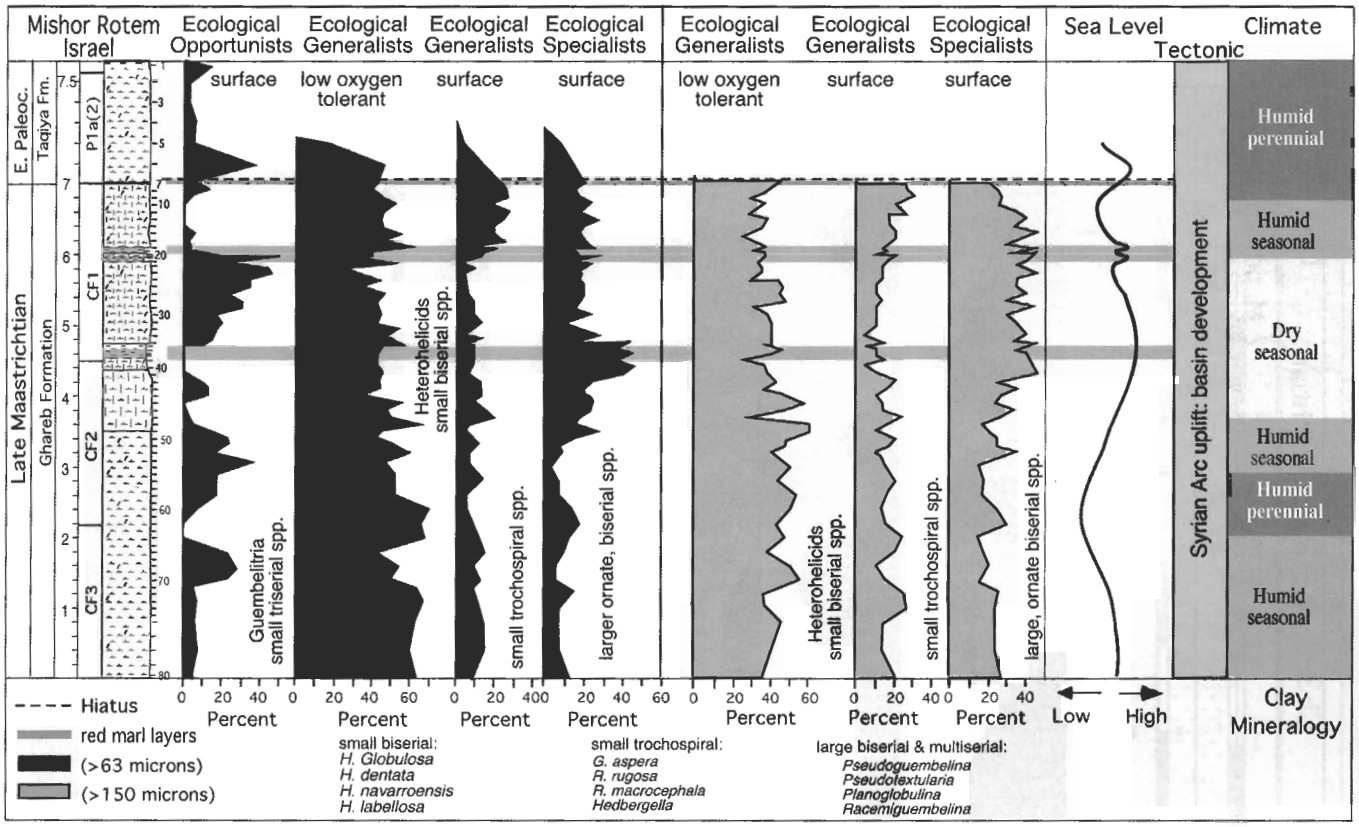

FIGURE 11. Late Maastrichtian to early Danian planktic foraminifera grouped into ecological opportunists, generalists and specialists representing life modes and depth habitats at Mishor Rotem, Israel. Sea level changes and climatic interpretation based on bulk rock and clay mineralogy from Adatte and others, (in press). Grey lines mark red marl layers, dashed line at K/T boundary marks hiatus.

itria peaks average only 5–10% (Abramovich and Keller, 2002). Outside the eastern Tethys, *Guembelitria* is generally rare or absent in late Maastrichtian age sediments, except for very shallow nearshore environments (e.g., Alabama, Texas, Denmark, southern Tunisia, and Madagascar, Keller and others, 2002c; Abramovich and others, 2002), and *G. dammula* is abundant in the upper bathyal environment of eastern Bulgaria (Adatte and others, 2002a).

Guembelitria cretacea is generally abundant during times of high ecological stress when few other species thrive, and it has therefore been labeled an opportunist or disaster species (Keller and others, 2002b). This species is present in very low frequencies (<1%) in late Maastrichtian foraminiferal assemblages of normal open marine environments, but more abundant (10–20%) in shallow nearshore environments. However, during crisis conditions when other species populations show reduced abundances and diversity and many species disappeared altogether, *Guembelitria* spp. tend to produce opportunistic blooms, as is well known for the K/T boundary clay and early Danian (Keller and others, 2002b).

The persistent and relatively high abundances of this species group in shallow or nearshore areas during the late Maastrichtian suggest a high tolerance for salinity, nutrient and temperature fluctuations. In southern Tunisia (Seldja), *Guembelitria* dominance is associated with a warm humid climate, high rainfall, low salinity, high organic matter influx from nearby terrestrial areas, and low oxygen bottom water conditions (Keller and others, 1998). *Guembelitria* abundances tend to show opposite trends to *Rugoglobigerina, Heterohelix navaroensis* and *H. globulosa* in southern Tunisia and central Egypt, as also observed in the Negev at Mishor Rotem (Fig. 12).

COMPARISON OF SOUTHERN ISRAEL AND CENTRAL EGYPT

The unusually impoverished planktic foramniferal assemblages of the southern Negev, Israrel, can be compared with the even more impoverished assemblages from Qreiya in central Egypt. Both localities show similar aspects with unusually high abundances of *Guembelitria* and low oxygen tolerant biserial species during the late Maastrichtian (Figs. 11, 12), although in central Egypt *Guembelitria* abundances are much higher (75–90%) and comparable to abundances in the early Danian after the K/T mass extinction (Keller, 2002). The *Guembelitria* peaks at the Qreiya section appear to be correlative with the smaller (30–40%) peaks in the Mishor Rotem section (Fig. 13) and elsewhere in southern Israel (Abramovich and others, 1998). At times of low *Guembelitria* abundance, small biserial species dominate, indicating low oxygen conditions. Ecological generalists are rare, except during the warming of the uppermost Maastrichtian zone CF1 when the small trochospiral species (including *Plummerita hantkeninoides* and *R. reicheli*) reach peak abundance of 40% (Fig. 12). Rugoglobigerinids tend

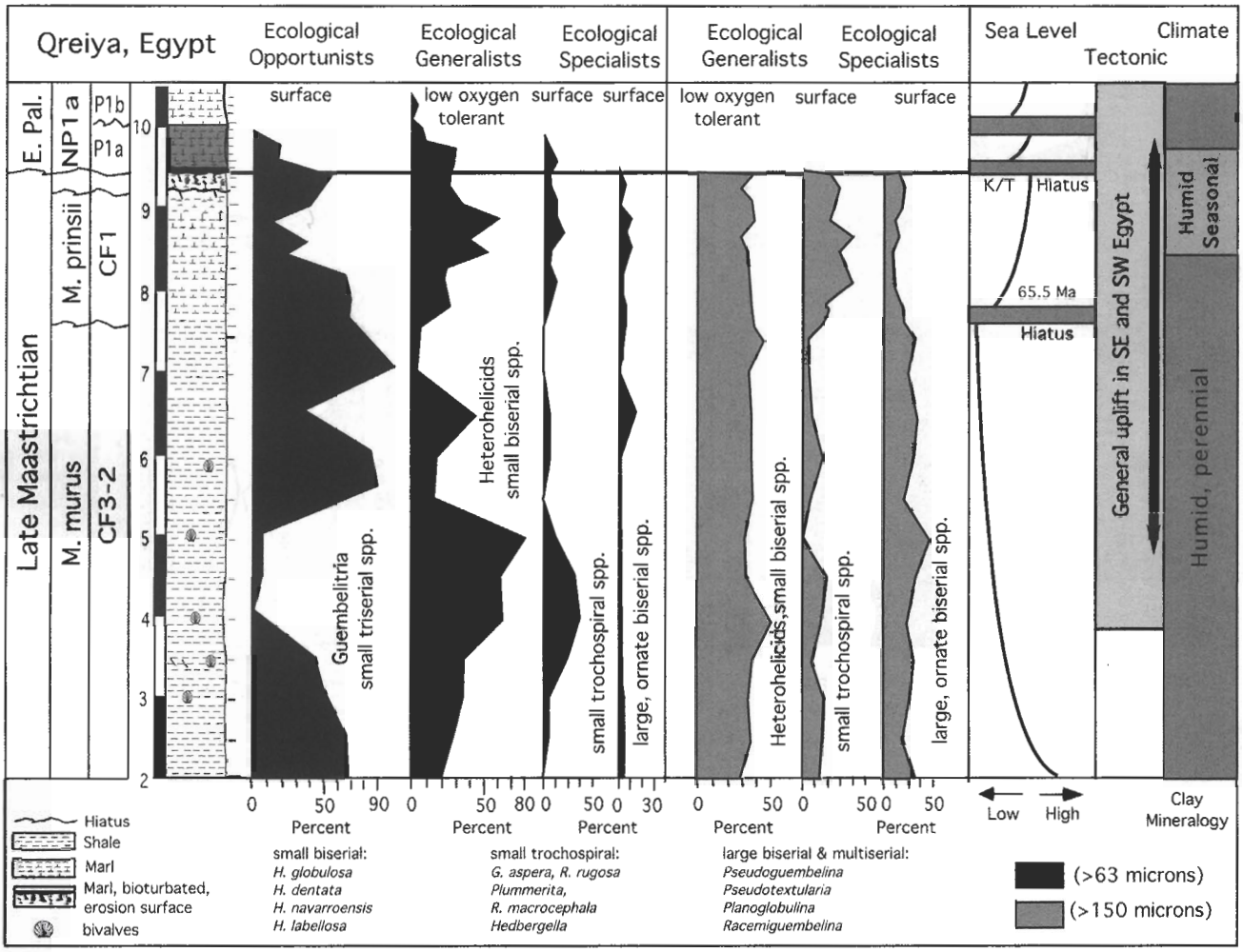

FIGURE 12. Late Maastrichtian to early Danian planktic foraminifera grouped into ecological opportunists, generalists and specialists representing life modes and depth habitats at Qreiya, Egypt. Sea level changes, tectonic and climatic interpretations from Keller and others (2002).

to be most abundant during climate warming, and the peak abundance in CF1 in Egypt may reflect the global warming between 65.4–65.2 Ma (Kucera and Malmgren, 1998; Li and Keller, 1998a). The absence of this peak abundance at Mishor Rotem suggests that the upper part of zone CF1 is missing at the undulating erosional surface that marks the top of the Ghareb Formation and K/T boundary (Fig. 11).

Carbon isotope data of the Qreiya section show a sharply decreased surface-to-deep gradient correlative with maximum *Guembelitria* abundance (Fig. 13), similar to the decreased gradient associated with *Guembelitria* dominance after the K/T boundary event. At the K/T boundary these isotopic and biotic patterns are generally interpreted as evidence of a productivity crash after the mass extinction (Keller and Lindinger, 1989; Zachos and others, 1989; Barrera and Keller, 1994). By analogy, the Qreiya section experienced a similar productivity crash in the late Maastrichtian, though unlike the K/T boundary there is no evidence of a sudden catastrophe (e.g., impact or volcanism). The Qreiya section thus suggests that the planktic foraminiferal response to the K/T catastrophe was not unique, but followed a similar pattern of response to severe environmental disturbances that is expressed in high *Guembelitria* abundances. Moreover, the southern Israel sections indicate that this late Maastrichtian disturbance was widespread and at least regional encompassing the eastern Tethys, though it may even be global, as suggested by recent data from Bulgaria and Madagascar (Adatte and others, 2002, Abramovich and others, 2002) that reveal similar *Guembelitria* dominance during the late Maastrichtian.

MAASTRICHTIAN PALEOECOLOGY OF THE EASTERN TETHYS

Although the ultimate cause of the late Maastrichtian environmental disturbance in the eastern Tethys is still unclear, a major contributing factor appears to be the strong global cooling at about 65.5 Ma accompanied by a lower sea level and followed by rapid warming and a sea level rise between 65.45 and 65.2 Ma (Barrera, 1994; Li and Keller, 1998a,b). The warming is associated with generally improved environmental conditions (e.g., higher species diversity, decrease in ecological opportunists and increase in ecological generalists and specialists), whereas the cooling (and lower sea level) is associated with the opposite. Eustatic sea level changes, coupled with the tectonically active basin and ridge

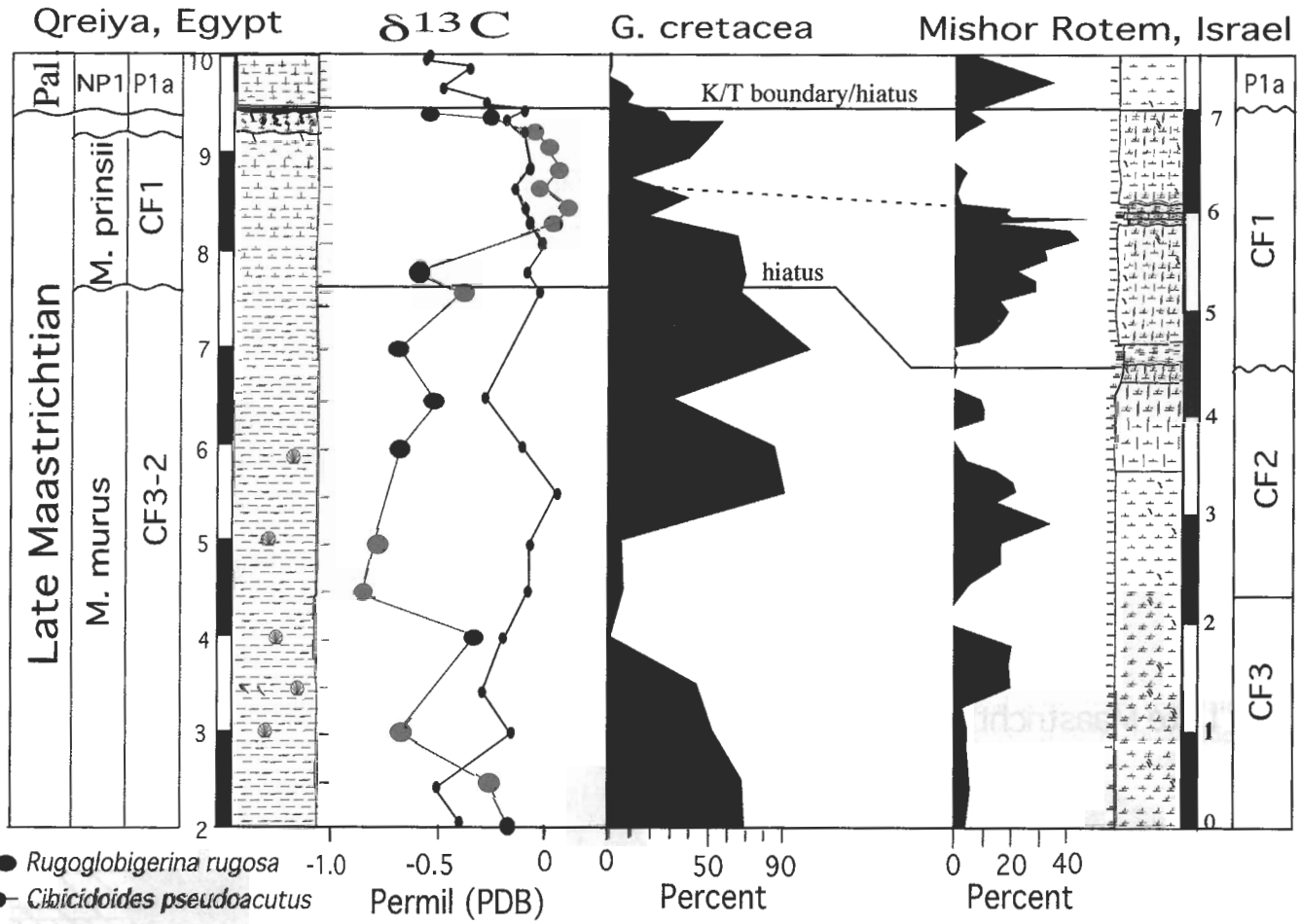

FIGURE 13. Late Maastrichtian carbon isotope values of benthic and planktic foraminifera at Qreiya, Egypt (Keller and others, 2002c), compared with occurrences of opportunistic blooms of *Guembelitria* at the Qreiya and Mishor Rotem sections. Note the inverse surface-to-deep $\delta^{13}C$ gradient in zone CF3-2 is similar to the productivity crash observed in K/T boundary sections in low and middle latitudes (see text for discussion).

paleotopography of the Syrian Arc in the eastern Tethys, would have affected the paleobathymetry of both the deeper Mishor Rotem section of the Negev and the shallower Qreiya section of central Egypt with attendant changes in circulation and upwelling regimes (Fig. 14).

In central Egypt, the Qreiya section was located in a relatively shallow marginal sea at a depth of about 100–200 m (Fig. 1a) (Hendriks and others, 1987; Luger, 1988; Schnack and Luger, 1998; Keller and others, 2002c). A sea level lowering of 50 m (Li and others, 1999) would have severely restricted circulation, perhaps isolated basins by topographic highs, resulting in salinity, oxygen and nutrient changes. A possible scenario for the high-stress planktic foraminiferal fauna of this locality is shown in Figure 14a. Sediment deposition likely occurred in a relatively shallow basin (100–200 m) with restricted bottom circulation, as suggested by dysaerobic bottom waters indicated by generally low diversity assemblages consisting of *Globobulimina, Uvigerina, Nodosaria* and *Cibicidoides.* The surface mixed layer (~50 m) is dominated by the opportunist *Guembelitria* (~75–90%) to the near-exclusion of most other species, and suggests high stress possibly due to high detrital influx from nearby continental areas (high quartz and plagioclase, Keller and others, 2002c). The dominance of subsurface dwelling, low-oxygen-tolerant, biserial species suggests reduced watermass stratification with an expanded oxygen minimum zone and dysaerobic (oxygen depleted) zone. This is also indicated by the notable absence of the deeper dwelling species of the globotruncanid group (<1%) that thrived in well-stratified aerobic waters. The generally low productivity indicated by carbon isotopes (Fig. 13), low species diversity (Fig. 9), and assemblages consisting of ecological generalists and opportunists, is also reflected by the low organic content in sediments (≤0.5%, Keller and others, 2002c).

Planktic foraminiferal assemblages indicate that similar, though less severe, stress conditions also prevailed at the Mishor Rotem section in southern Israel. The main difference between these sections is the greater paleodepth at Mishor Rotem, where benthic foraminifera indicate deposition in an upper bathyal environment at about 300–500 m depth. Diverse benthic assemblages dominated by rotaliids, including *Cibicidoides, Stensioiina, Pullenia* and *Planulina,* indicate aerobic bottom conditions controlled by deep water circulation (Keller, 1992; this study). Planktic foraminiferal assemblages are of slightly higher diversity than at Qreiya, but also indicate reduced watermass stratification. The surface assemblage consists of small planispiral and

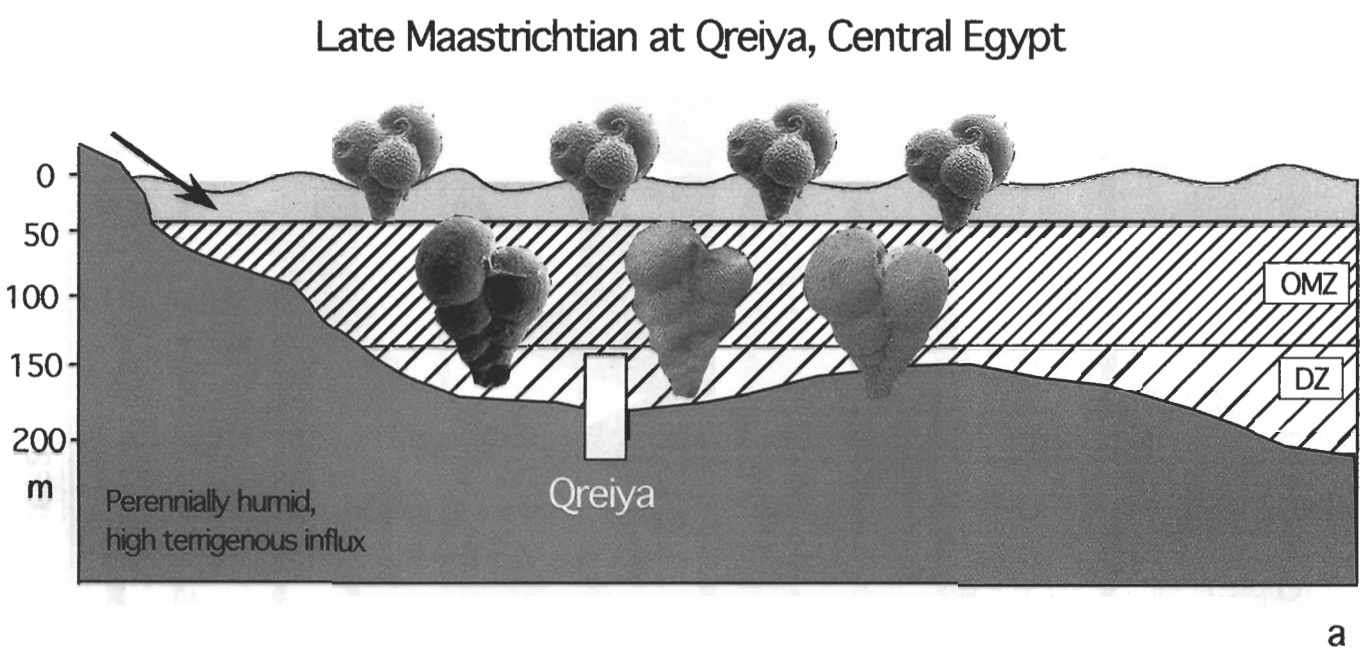

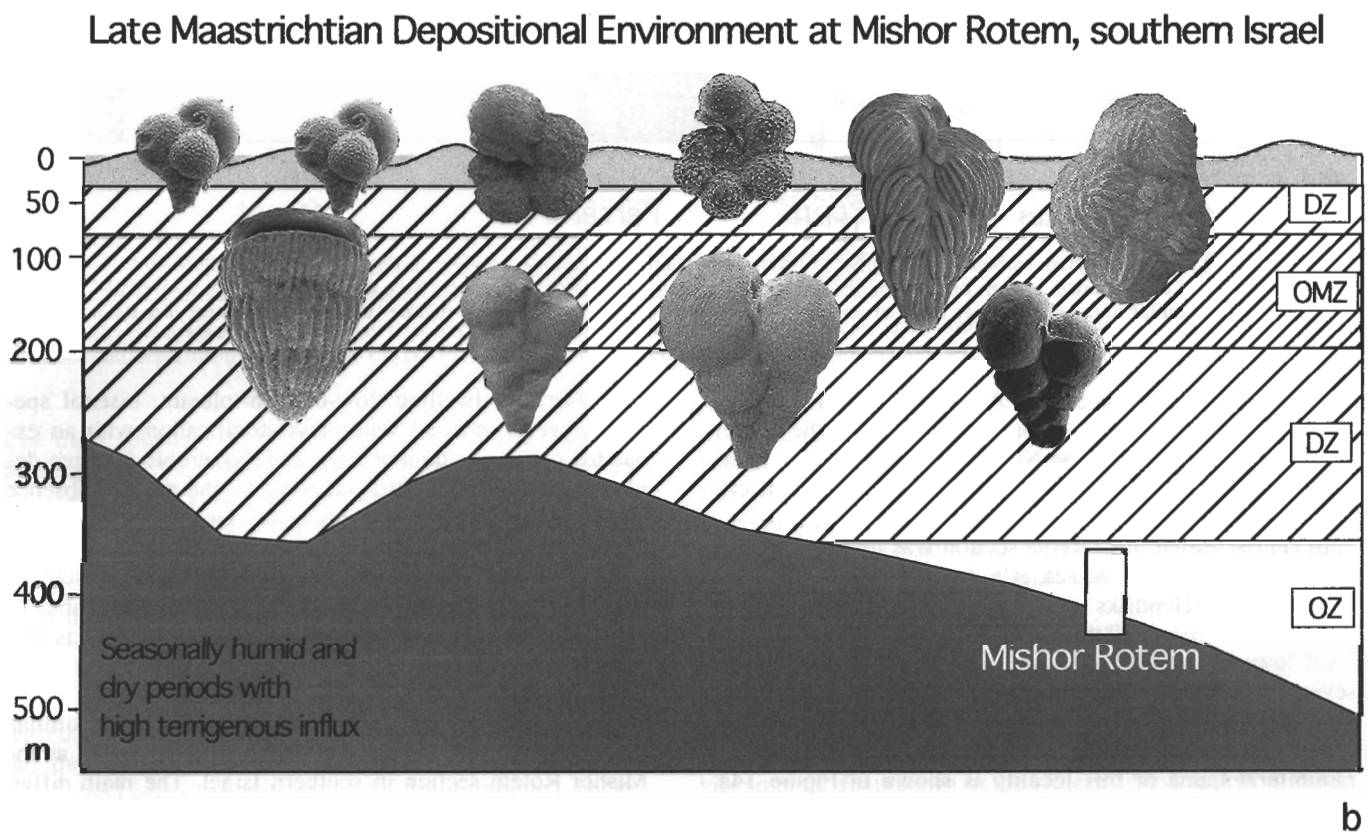

FIGURE 14a. Model of late Maastrichtian paleoecologic conditions at Qreiya, Egypt, showing restricted circulation and poorly stratified watermass with dysaerobic (DZ) bottom waters populated by low diversity benthic assemblages (e.g., *Globobulimina, Uvigerina, Nodosaria, Cibicidoides*), an expanded oxygen minimum zone (OMZ) populated by low oxygen tolerant small biserial species, and mixed surface water populated by the opportunist or disaster species *Guembelitria*. Perennially humid climate and high terrigenous influx result in low primary productivity, nutrient and salinity fluctuations which favor blooms of opportunistic species.

FIGURE 14b. Model of late Maastrichtian paleoecologic conditions at Mishor Rotem, Israel, showing less restricted bottom circulation and hence aerobic bottom waters with diverse benthic assemblages dominated by rotaliids (*Cibicidoides, Stensioina, Pullenia, Planulina*). The upper watermass is poorly stratified with a well-developed oxygen minimum zone (OMZ) and dysaerobic zone (DZ) populated by low-oxygen-tolerant, small and large biserial species. Primary productivity in the mixed surface layer is variable with blooms of the opportunist or disaster species *Guembelitria* at times of low productivity, but high nutrient influx from terrestrial areas during seasonally humid climates.

trochospiral ecological generalists (*G. aspera, Hedbergella, R. rugosa*), some biserial specialists (*Pseudoguembelina, Pseudotextularia, Planoglobulina*), and three *Guembelitria* blooms during the late Maastrichtian (Fig. 11). These surface assemblages suggest variable stress conditions possibly related to salinity and nutrient variations, as supported by high terrigenous influx, similar to Qreiya in central Egypt (Adatte and others, in press). The subsurface assemblage is dominated by low-oxygen-tolerant, small, biserial heterohelicids that indicate oxygen-depleted waters (oxygen minimum and dysaerobic zone, Fig. 14b). Similar to Qreiya, the deeper dwelling globotruncanids are nearly absent (~1–2%, Fig. 8) indicating disruption of normal water mass stratification and reduction or elimination of intermediate depth habitats as a result of an expanding oxygen minimum zone.

The vertical extent of the oxygen minimum zone (OMZ) depends on primary productivity in surface waters. At times of high primary productivity, the OMZ expands to the detriment of species requiring well-aerated waters and favoring low-oxygen-tolerant heterohelicids. In an analysis of pre-Maastrichtian upwelling systems in Israel, Almogi-Labin and others (1993) suggested that high abundance of the surface dweller *Globigerinelloides* reflects high surface-water productivity and implies intensification and shallowing of the OMZ. However, a stable isotope study of *Globigerinelloides* at the Cenomanian-Turonian transition of Pueblo, Colorado, indicates that high abundances (>35%) of *Globigerinelloides* thrived in low-salinity waters that excluded *Guembelitria* (Keller and Pardo, 2004). At the Mishor Rotem and Qreiya sections, *Globigerinelloides* are a minor component (1–8%), except in the upper part of zone CF1 where they reach 20%. By this proxy, low surface salinity is not responsible for the expanded OMZ or the high abundance of *Guembelitria.* On the other hand, low surface productivity (Fig. 13) is indicated by low carbon isotope values, low TOC (Keller and others, 2002c), low surface diversity and deposition of chalk and limestones in southern Israel. In view of these observations, the expanded OMZ is probably more likely a function of increased water mass stratification and detrital influx from adjacent continental areas.

DISCUSSION AND CONCLUSIONS

Late Maastrichtian planktic foraminiferal assemblages of Mishor Rotem reveal high-stress environmental conditions in southern Israel that resulted in low species diversity, the near absence of globotruncanids, dominance of heterohelicids, and intermittent blooms of the opportunists *Guembelitria* (Figs. 11–12). Similarly impoverished and high-stress assemblages were earlier reported from four other sections in southern Israel by Abramovich and others (1998), who relate these to global paleoenvironmental changes, including changes in productivity and climate. Global climate changes very likely account for the long-term decrease in species richness, but probably not for the anomalous peaks in *Guembelitria* and the very low abundance of keeled globotruncanids that appear to be more particular to the eastern Tethys.

What role, if any, did the red marl layers of the Mishor Rotem section play in the accelerated decline of the late Maastrichtian assemblages in southern Israel? Data from the Mishor Rotem section suggest that they represent times of relatively optimum conditions for the region, as suggested by the absence of *Guembelitria* blooms (Fig. 12). Although ecological generalists, *H. navarroensis, H. globulosa, H. dentata, R. rugosa* and *R. macrocephala* show decreased abundances (Figs. 7, 8), these are not unique and cannot be tied to the red marl layers with confidence. Lithologically, the laminated red marls represent condensed deposition under locally elevated sea levels (e.g., tectonic effects) relative to the chalks and marly limestones above and below, as also suggested by high concentrations of platinum group elements (Adatte and others, in press). However, the anomalous trace element concentrations, including Ir, and the fact that an Ir anomaly has also been observed in Oman at this stratigraphic interval (Ellwood and others, 2003), indicates that a pre-K/T impact cannot be ruled out.

In central Egypt, planktic foraminiferal assemblages indicate even higher stress conditions in the late Maastrichtian than in southern Israel, as suggested by *Guembelitria* blooms dominating (75–90%) the foraminiferal population. These assemblages are accompanied by strongly negative $\delta^{13}C$ values that suggest a breakdown of the surface-to-bottom gradient of the $^{13}C/^{12}C$ ratio (Fig. 13, Keller, 2002). This breakdown in primary productivity occurred during global climate cooling in CF3 and a sea level regression that peaked at 65.5 Ma and probably accounts for a widespread hiatus at this time (Li and others, 2000; Adatte and others, 2002a, b).

However, at similar paleodepths in Tunisia these unsual *Guembelitria* blooms are absent, though slightly increased abundances (5–10%) are observed in the upper zone CF3 and in CF1 (e.g., the middle to outer neritic Elles section and outer neritic to upper bathyal El Kef section; Abramovich and Keller, 2002; Li and Keller, 1998c). This suggests that the environmental conditions of the eastern Tethys did not extend far to the west (no data available for Libya) and no *Guembelitria* blooms have been observed in Spain. However, unusual *Guemblitria* dominance was observed in the Bjala section in eastern Bulgaria where *Guembelitria cretacea* is common (~10%) in the upper zone CF1 and the larger *G. dammula* dominates the assemblages by 60–80% (Adatte and others, 2002b). In Madagascar, *Guembelitria dammula* is common and *G. cretacea* dominant during the late Maastrichtian. It is still unclear what relationship, if any, these *Guembelitria* dominances have to the eastern Tethys and further studies are necessary to determine the environmental conditions in which *G. dammula* thrived.

The high-stress conditions exhibited by planktic foraminiferal assemblages in the eastern Tethys are at least partly related to regional paleobathymetry of the tectonically active Syrian Arc (Fig. 1) coupled with global climate and sea level changes. The paleorelief of intra-shelf and intra-slope basins of the Syrian Arc with their differential rates of subsidence and sedimentation, and active folding and faulting, likely controlled the intensity of circulation, upwelling, watermass stratification and the extent of the oxygen minimum zone (Reiss, 1988), though the decreasing sea level associated with global cooling during the late Maastrichtian probably exacerbated these conditions. However, volcanism and impacts cannot be ruled out as primary causes for the high-stress conditions, particularly in view of the accumulating

evidence of at least one pre-K/T impact (e.g., northeastern Mexico, Oman, Israel; Keller and others, 2002a, 2003; Ellwood and others, 2003).

ACKNOWLEDGEMENTS

I'm grateful to Sigal Abramovich, Thierry Adatte, Wolfgang Stinnesbeck and Chaim Benjamini for field and laboratory assistance, as well as many discussions and Alessadro Montanari, Hans Jurgen Hansen and Wolfgang Weitschat for help in identifying the amber spherules. I thank the reviewers Mark Leckie and O.W. Haig for their helpful comments. This study was supported in part by NSF BSF Award # 19800425.

REFERENCES

ABRAMOVICH, S., ALMOGI, L. A., and BENJAMINI, C., 1998, Decline of the Maastrichtian pelagic ecosystem based on planktic foraminifera assemblage change; implication for the terminal Cretaceous faunal crisis: Geology v. 26, no. 1, p. 63–66.

———, and KELLER, G., 2002, High stress late Maastrichtian paleoenvironment: Inferences from planktic foraminifera in Tunisia: Palaeogeography, Palaeoclimatology, Palaeoecology, v. 178, p. 145–164.

———, ———, ADATTE, T., STINNESBECK, W., HOTTINGER, L., STUEBEN, D., BERNER, Z., RAMANIVOSOA, B., and RANDRIAMANANTENASOA, A., 2002, Age and Paleoevironment of the Maastrichtian to Paleocene of the Mahajanga Basin, Madagascar: a multidisciplinary approach: Marine Micropaleontology, v. 47, no. 1–2, p. 17–20.

———, ———, STUEBEN, D., and BERNER, Z., 2003, Characterization of late Campanian and Maastrichtian planktic foraminiferal depth habitats and vital activities based on stable isotopes: Palaeoclimatology, Palaeoecology, Palaeogeography, 2002, p. 1–29.

ADATTE, T., KELLER, G., BURNS, S., STOYKOVA, K. H., IVANOV, M. I., VANGELOV, D., KRAMER, U., and STUEBEN, D., 2002a, Paleoenvironment across the Cretaceous-Tertiary transition in eastern Bulgaria: Geological Society of America, Special Paper 356, p. 231–252.

———, ———, and STINNESBECK, W., 2002b, Late Cretaceous to Early Paleocene climate and sea-level fluctuations: Palaeoclimatology, Palaeoecology, Palaeogeography, v. 178, p. 165–196.

———, ———, STUEBEN, D., HASTINGS, M., KRAMAR, U., STINNESBECK, W., ABRAMOVICH, S., and BENJAMINI, C., in press, Late Maastrichtian and K/T paleoenvironment of the eastern Tethys (Israel): Mineralogy, Trace and Platinum group elements, biostratography and formal turnover: Geological Society of France.

ALMOGI-LABIN, A., FLEXER, A., HONIGSTEIN, A., ROSENFELD, A., and ROSENTHAL, E., 1990, Biostratigraphy and tectonically controlled sedimentation of the Maastrichtian in Israel and adjacent countries: Revista Espanola de Paleontologia, v. 5, p. 41–52.

———, BEIN, A., and SASS, E., 1993, Late Cretaceous upwelling system along the southern Tethys margin (Israel): interrelationship between productivity, bottom water environments and organic matter preservation: Paleoceanography, v. 8, p. 671–690.

BANDEL, K., SHINAC, R., and WEITSCHAT, W., 1997, First insect inclusions from the amber of Jordan (Mid Cretaceous): Mitthandlungen Geologie und Paleontologie Institute, University of Hamburg, v. 80, p. 213–223.

BARRERA, E., 1994, Global environmental changes preceding the Cretaceous-Tertiary boundary: Early-upper Maastrichtian transition: Geology, v. 22, p. 877–880.

———, and KELLER, G., 1994, Productivity across the Cretaceous/Teriary boundary in high latitudes: Geological Society of America Bulletin, v. 106, p. 1254–1266.

BERGGREN, W. A., KENT, D. V., SWISHER, C. C., III and AUBRY, M.-P., 1995, A revised Cenozoic geochronology and chronostratigraphy, *in* Berggren, W.A., Kent, D.V., Aubry, M.-P. and Hardenbol, J., (eds), Geochronology, Time Scales and Global Stratigraphic Correlation: Society for Sedimentary Geology, Special Publication 54, p. 129–212.

BOERSMA, A., and PREMOLI SILVA, I., 1989, Atlantic Paleogene biserial heterohelicid foraminifera and oxygen minima: Paleoceanography, v. 4, no. 3, p. 271–286.

BOSWORTH, W., GUIRAUD, R., and KESSLER, L.G., 1999, Late Cretaceous (ca. 84 Ma) compressive deformation of the stable platform of northeast Africa (Egypt): Far-field stress effects of the "Santonian event' and origin of the Syrian arc deformation belt: Geology, v. 27, no 7, p. 633–636.

COURTILLOT, V., JAEGER, J.-J., YANG, Z., FERAUD, G., and HOFMANN, C., 1996, The influence of continental flood basalts on mass extinctions: Where do we stand?: Geologic Society of America, Special Paper 307, p. 513–526.

D'HONDT, S., and ARTHUR, M. A., 1995, Interspecific variation in stable isotopic signals of Maastrichtian planktic foraminifera: Paleoceanography, v. 10, p. 123–135.

ELLWOOD, B. B., MACDONALD, W. D., WHEELER, C., and BENOIST, S. L., 2003, The K-T boundary in Oman: identified using magnetic susceptibility field measurements with geochemical Confirmation: Earth and Planetary Science Letters, v. 206, p. 529–540.

HENDRIKS, F., LUGER, P., BIWITZ, J., and KALLENBACH, H., 1987, Evolution of the depositional environments of SE Egypt during the Cretaceous and lower Tertiary: Berliner Geowissenschaftliche Abhandlungen (A), v. 75, p. 49–82.

HOFFMANN, C., FERAUD, G., and COURTILLOT, V., 2000, 40Ar/39Ar dating of mineral separates and whole rocks from the Western Ghats lava pile: further constraints on duration and age of Deccan traps: Earth and Planetary Science Letters, v. 180, p. 13–27.

KELLER, G., 1988, Extinction, survivorship and evolution of planktic foraminifera across the Cretaceous/Teriary boundary at El Kef Tunisia: Marine Micropaleontology, v. 13, p. 239–263.

———, 1989, Extended Cretaceous/Teriary boundary extinctions and delayed population change in planktonic foraminifera from Brazos River, Texas: Paleoceanography, v. 4, p. 287–332.

———, 1992, Paleoecologic response of Tethyan benthic foraminifera to the Cretaceous-Tertiary boundary transtion: Studies in Benthic Foraminifera, BENTHOS '90, Sendai 1990, Tokai University Press, p. 77–91,

———, 2001, The end-Cretaceous mass extinction in the marine realm: year 2000 assessment: Planetary and Space Science, v. 49, p. 817–830.

———, 2002, *Guembelitria* dominated planktic foraminiferal assemblages mimic early Danian in central Egypt: Marine Micropaleontology, v. 47, p. 71–99.

———, and BENJAMINI, C., 1991, Paleoenvironment of the eastern Tethys in the Early Paleocene: Palaios, v. 6, p. 439–464.

———, and LINDINGER, M., 1989, Stable isotopes, TOC and CaCO3 records across the Cretaceous-Tertiary boundary at El Kef, Tunisia: Paleogeography, Paleoclimatology, Paleoecology, v. 73, p. 243–265.

———, LI, L., and MACLEOD, N., 1995, The Cretaceous/Tertiary boundary stratotype section at El Kef, Tunisia: How catastrophic was the mass extinction? Paleogeography, Paleoclimatololgy, Paleoecology v. 119, p. 221–254.

———, and PARDO, A., 2004, Age and paleoenvironment of the Cenomanian-Turonian global stratotype section and point at Pueblo, Colorado: Marine Micropaleontology, in press.

———, BARRERA, E., SCHMITZ, B., and MATSSON, E., 1993, Gradual mass extinction, species survivorship, and long term environmental changes across the Cretaceous-Tertiary boundary in high latitudes: Geological Society of America Bulletin, v. 105, p. 979–997.

———, ADATTE, T., STINNESBECK, W., STUBEN, D., KRAMAR, U., BERNER, Z., LI, L., and PERCH-NIELSEN, K., 1998, The Cretaceous-Tertiary transition in the shallow Saharan platform of southern Tunisia: Geobios, v. 30, no. 7, p. 951–975.

———, ———, ———, AFFOLTER, M., SCHILLI, L., and LOPEZ-OLIVA, J.G., 2002a, Multiple spherule layers in the late Maastrichtian of northeastern Mexico: Geological Society of America, Special Publication 356, p. 145–162.

———, ———, ———, W., LUCIANI, V., KAROUI, N., and ZAGHBIB-TURKI, D., 2002b, Paleobiogeography of the Cretaceous-Tertiary mass extinction in planktic foraminifera: Palaeogeography, Palaeoclimatololgy, Palaeoecology, v. 178, p. 257–298.

———, ———, BURNS, S. J., and TANTAWY, A. A., 2002c, High-

stress paleoenvironment during the late Maastrichtian to early Paleocene in Central Egypt: Palaeogeography, Palaeoclimatololgy, Palaeoecology, v. 187, p. 35–60.

———, STINNESBECK, W., ADATTE, T., and STUEBEN, D., 2003, Multiple impacts across the Cretaceous-Tertiary boundary: Earth-Science Reviews, 62, p. 327–363.

KUCERA, M., and MALMGREN, B.A., 1998, Terminal Cretaceous warming event in the mid-latitude South Atlantic Ocean: evidence from poleward migration of *Contusotruncana contusa* (planktonic foraminifera) morphotypes: Palaeogeography, Palaeoclimatology, Palaeoecology, v. 138, p. 1–15.

LECKIE, R. M., 1987, Paleoecology of mid-Cretaceous planktonic foraminifera: a comparison of open ocean and epicontinental sea assemblages: Micropaleontology, v. 33, p. 264–176.

LI, L., and KELLER, G., 1998a, Abrupt deep-sea warming at the end of the Cretaceous: Geology, v. 26, p. 995–99.

——— and ———. 1998b, Maastrichtian climate, productivity and faunal turnovers in planktic foraminifera in South Atlantic DSDP Sites 525 and 21. Marine Micropaleontology, v. 33, p. 55–86.

——— and ———, 1998c, Maastrichtian diversification of planktic foraminifera at El Kef and Elles, Tunisia: Eclogae Geologicae Helvetiae v. 91, p. 75–102.

———, ———, and STINNESBECK, W., 1999, The Late Campanian and Maastrichtian in northwestern Tunisia: Paleoenvironmental inferences from lithology, macrofauna and benthic foraminifara: Cretaceous Research, v. 20, p. 231–252.

———, ———, ADATTE, T., and STINNESBECK, W., 2000, Late Cretaceous sea level changes in Tunisia: a multi-disciplinary approach: Journal of the Geological Society of London, v. 157, p. 447–458.

LOPEZ-OLIVA, J. G., and KELLER, G., 1996, Age and stratigraphy of near-K/T boundary siliciclastic deposits in northeastern Mexico: Geological Society of America, Special Paper 307, p. 227–242.

LUCIANI, V., 1997, Planktonic foraminiferal turnover across the Cretaceous-Teriary boundary in the Vajont valley (Southern Alps, northern Italy): Cretaceous Research, v. 18, p. 799–821.

———, 2002, High resolution planktonic foraminiferal analysis from the Cretaceous/Tertiary boundary at Ain Settara (Tunisia): Evidence for an extended mass extinction: Palaeogeography, Palaeoclimatololgy, Palaeoecology, v. 178, p. 299–320.

LUGER, P., 1988, Maastrichtian to Paleocene facies evolution and Cretaceous/Tertiary boundary in middle and southern Egypt: Revista Espanola de Micropaleontologia, Numero Extraordinario, p. 83–90.

———, and GRÖSCHKE, M., 1989, Late Cretaceous ammonites from the Wadi Qena area in the Egyptian Eastern Desert: Palaeontology, v. 32, no. 2, p. 355–407.

MACLEOD, K., G., HUBER, B. T., PLETSCH, T., RÖHL, U., and KUCERA, M., 2001, Maastrichtian foraminiferal and paleoceanographic changes on Milankovitch timescales: Paleoceanography, v. 16, no. 2, p. 133–154.

MACLEOD, N., and KELLER, G., 1991, How complete are Cretaceous/Tertiary boundary sections? A chronostratigraphic estimate based on graphic correlation: Geological Society of America, Bulletin, v. 103, p. 1439–1457.

MAGARITZ, M., MOSHKOVITZ, S., BENJAMINI, C., HANSEN, H. J., HAKANSSON, E., and RASMUSSEN, K.L., 1985, Carbon isotope-, bio and magnetostratigraphy across the Cretaceous-Tertiary boundary in the Zin Valley, Negev, Israel. Newsletter: Stratigraphy, v. 15, no. 2, p. 100–113.

MALMGREN, B. A., 1991, Biogeographic patterns in terminal Cretaceous planktonic foraminifera from Tethyan and warm transitional waters: Marine Micropaleontology, v. 18, p. 73–99.

MASTERS, B. A., 1997, El Kef blind test II results: Marine Micropaleontology, v. 29, p. 77–79.

NEDERBRAGT, A. J., 1991, Late Cretaceous biostratigraphy and development of *Heterohelicidae* (planktic foraminifera): Micropaleontology, v. 37, p. 329–372.

———, 1998, Quantitative biogeography of late Maastrichtian planktic foraminifera: Micropaleontology, v. 44, p. 385–412.

OLSSON, R.K., 1997, El Kef blind test III results: Marine Micropaleontology, v. 29, p. 80–84.

———, WRIGHT, D. J., and MILLER, K. G., 2001, Paleobiogeography of *Pseudotextularia elegans* during the latest Maastrichtian global warming event: Journal of Foraminiferal Research, v. 31, no. 3, p. 275–282.

ORUE-ETXEBARRIA, X., 1997, El Kef blind test IV results: Marine Micropaleontology, v. 29, p. 85–88.

PARDO, A., ORTIZ, N., and KELLER, G., 1996, Latest Maastrichtian and K/T boundary foraminiferal turnover and environmental changes at Agost, Spain, *in* MacLeod N., and Keller, G. (eds.), The Cretaceous-Tertiary Boundary Mass Extinction: Biotic and Environmental Events: W. W. Norton & Co., New York, p. 155–176.

REISS, Z., 1988, Assemblages from a Senonian high productivity sea, *in* Benthos '86. Revue Paleobiology, Special Volume 2, p. 323–332.

ROSENFELD, A., FLEXER, A., HONIGSTEIN, A., ALMOGI-LABIN, A., and DVORACHEK, M., 1989, First report on a Cretaceous/Tertiary boundary section at Makhtesh Gadol, southern Israel: Neues Jahrbuch Geologie Paleontologie Mithandlungen, v. 8, p. 474–488.

ROSENTHAL, E., WEINBERGER, G., ALMOGI-LABIN, A., and FLEXER, A., 2000, Late Cretaceous-early Tertiary development of depositional basins in Samaria as a reflection of eastern Mediterranean tectonic evolution: American Association of Petroleum Geologists, Bulletin, v. 84, p. 997–1014.

SCHNACK, K., and LUGER, P., 1998, Facies and structural evolution during the Maastrichtian and Paleocene in the Kharga uplift area and adjacent areas (Western Desert, SW-Egypt): Zuhandlungen Geologie Palaeontologie, v. 1, p. 311–351.

SMIT, J., 1999, The global stratigraphy of the Cretaceous-Tertiary boundary impact ejecta: Annual Reviews in Earth and Planetary Sciences, v. 27, p. 75–113.

SPEIJER, R. P., 1994, Extinction and recovery patterns in benthic foraminiferal paleocommunities across the Cretaceous/Paleogene and Paleocene/Eocene boundaries: Geologica Ultraiectina, Medelingen van de Faculteit Aardwetenschappen, Universiteit Utrecht, 190 p.

TANTAWY, A. A., 2003, Calcareous nannofossil biostratigraphy and paleoecology of the Cretaceous-Tertiary transition in the central eastern desert of Egypt: Marine Micropaleontology, v. 47, 323–356.

ZACHOS, J. C., ARTHUR, M. A., and DEAN, W. E., 1989, Geochemical evidence for suppression of pelagic productivity at the Cretaceous/Tertiary boundary: Nature, v. 337, no. 5, p. 41–64.

Received 28 October 2002
Accepted 22 May 2003